Aspects on the diagnostic performance of myocardial perfusion SPECT

Hedeer, Fredrik

2020

Document Version:
Publisher's PDF, also known as Version of record

Aspects on the diagnostic performance of myocardial perfusion SPECT

FREDRIK HEDEER
DEPARTMENT OF CLINICAL PHYSIOLOGY | FACULTY OF MEDICINE | LUND UNIVERSITY

Aspects on the diagnostic performance of myocardial perfusion SPECT

Aspects on the diagnostic performance of myocardial perfusion SPECT

Fredrik Hedeer

LUND
UNIVERSITY

Thesis for the degree of Doctor of Philosophy in Medical Science

Thesis advisors: Prof. Henrik Engblom, Prof. Håkan Arheden
and Assoc. Prof. Marcus Carlsson

Faculty opponent: Assoc. Prof. Antti Saraste, University of Turku

To be defended by due permission of the Faculty of Medicine, Lund University, Sweden at Segerfalksalen, BMC in Lund on Friday, June 5, 2020 at 13:00.

Organization LUND UNIVERSITY	**Document name** DOCTORAL DISSERTATION
	Date of issue June 5, 2020
Author(s): Fredrik Hedeer	Sponsoring organization

Title and subtitle

Aspects on the diagnostic performance of myocardial perfusion SPECT

Abstract

Coronary artery disease, leading to ischemic heart disease and myocardial infarction, is a major cause of mortality and a leading cause of heart failure worldwide. Different cardiac imaging methods are used for detection of myocardial ischemia and infarction as well as assessment of cardiac function, and play an important role for clinical management and decision making in these patients. Myocardial perfusion single-photon emission computed tomography (SPECT) is a widely used nuclear cardiac imaging method for diagnosing ischemic heart disease and myocardial infarction and for assessment of volumes and ejection fraction (EF) of the cardiac left ventricle (LV). Cardiac magnetic resonance imaging (CMR) is another imaging method considered to be the reference method for detection of myocardial infarction and cardiac function. The overall aim of this thesis was to further elucidate the diagnostic performance of myocardial perfusion SPECT (MPS) for detection of myocardial infarction and assessment of cardiac functional parameters, using CMR as the reference method.

Paper I investigated the diagnostic performance of MPS for assessment of LV volumes and LVEF and compared different MPS software, using CMR as the reference method. It was shown that MPS underestimates LV volumes compared to CMR whereas accuracy for assessment of LVEF was better. Precision was low for all measures. There were differences between the MPS software.

Paper II investigated the sensitivity and specificity of MPS with electrocardiography gated technique and a ^{99m}technetium labeled radiotracer for detection of myocardial infarction, using late gadolinium enhancement (LGE) CMR as the reference method. Gated MPS showed high sensitivity and specificity for infarct detection, only missing the smallest infarcts <3% of the LV mass.

Patients with a specific disturbance in the cardiac electrical conduction system, left bundle branch block (LBBB), are known to often have a specific tracer uptake pattern on MPS engaging the LV septal wall, mimicking perfusion defects seen in ischemia and infarction. The underlying pathophysiological mechanisms behind this MPS uptake pattern were investigated in **Paper III**. The results showed that typical MPS uptake pattern in patients with LBBB were mainly related to regional myocardial dyskinesia and wall thickening rather than myocardial fibrosis, stress-induced ischemia and ECG characteristics.

Paper IV sought to investigate the diagnostic performance of MPS for detection of myocardial infarction and assessment of LV volumes and LVEF, comparing a modern solid-state cadmium-zinc-telluride (CZT) detector gamma camera technique with a conventional gamma camera, using CMR as the reference method. The results showed a moderate sensitivity and high specificity for detection of infarcts >3% of the LV mass with no difference betweeen the gamma cameras. LV volumes were underestimated compared to CMR with a slighlty higher accuracy for the CZT compared to the conventional gamma camera and a relatively large impact on accuracy by the MPS software used.

In summary, the papers of this thesis showed a moderate to high sensitivity and high specificity for MPS to detect myocardial infarctions with no difference between modern and conventional gamma cameras. However, small infarcts were still missed by MPS. LV volumes were underestimated by MPS with low precision whereas accuracy for LVEF was better. The MPS software used had a higher impact on accuracy of LV volume and EF assessment than did type of gamma camera. It might be of value to take these results into consideration when interpreting an MPS study in a clinical setting.

Key words

Coronary artery disease, ischemic heart disease, myocardial infarction, myocardial perfusion SPECT, CMR

Classification system and/or index terms (if any)

Supplementary bibliographical information		**Language** English
ISSN and key title		**ISBN** 978-91-7619-934-3
Recipient's notes	**Number of pages** 69	Price
	Security classification	

Signature  Date 2020-04-28

Aspects on the diagnostic performance of myocardial perfusion SPECT

Fredrik Hedeer

LUND
UNIVERSITY

Faculty Opponent

Assoc. Prof. Antti Saraste
University of Turku
Turku, Finland

Evaluation Committee

Prof. Eva Nylander, Linköping University, Linköping, Sweden
Assoc. Prof. Sandra Lindstedt Ingemansson, Lund University, Lund, Sweden
Assoc. Prof. Johan Brandt, Lund University, Lund, Sweden

Coverphoto by Ebba Hedeer. Haväng, Österlen.

Department of Clinical Physiology, Faculty of Medicine, Lund University

ISBN 978-91-7619-934-3
ISSN 1652-8220

Printed in Sweden by Media-Tryck, Lund University
Lund 2020

Wer ein Warum zu leben hat, erträgt fast jedes Wie.
He who has a why to live can bear almost any how.

Friedrich Nietzsche, later used by Viktor Frankl

Table of Contents

List of publications

This thesis is based on the papers listed below. My contribution to the papers were as follows: Paper I – taking part in the design, collecting and analysing most of the data and writing the manuscript. Paper II – collecting and analysing some of the data and revised the manuscript. Paper III – taking part in the design, collecting and analysing most of the data and writing the manuscript. Paper IV – writing ethical application, taking part in the design, collecting and analysing most of the data and writing the manuscript.

I. **Hedeer F.**, Palmer J., Arheden H., Ugander M. Gated myocardial perfusion SPECT underestimates left ventricular volumes and shows high variability compared to cardiac magnetic resonance imaging – a comparison of four different commercial automated software packages. *BMC Med Imaging*. 2010 May 25; 10:10.

II. Carlsson M., **Hedeer F.**, Engblom H., Arheden H. Head-to-head comparison of a 2-day myocardial perfusion gated SPECT protocol and cardiac magnetic resonance late gadolinium enhancement for the detection of myocardial infarction. *J Nucl Cardiol*. 2013 Oct; 20(5):797-803.

III. **Hedeer F.**, Ostenfeld E., Hedén B., Prinzen FW., Arheden H., Carlsson M., Engblom H. To what extent are perfusion defects seen by myocardial perfusion SPECT in patients with left bundle branch block related to myocardial infarction, ECG characteristics and myocardial wall motion? *J Nucl Cardiol. 2020. Accepted.*

IV. **Hedeer F.**, Akil S., Oddstig J., Hindorf C., Arheden H., Carlsson M., Engblom H. Diagnostic performance of myocardial perfusion SPECT with a solid-state detector gamma camera compared to a conventional gamma camera for detection of myocardial infarction and assessment of left ventricular functional parameters using cardiac magnetic resonance as the reference method. *Manuscript.*

Publications not included in the thesis

Akil S., **Hedeer F.**, Oddstig J., Olsson T., Jögi J., Erlinge D., Carlsson M., Arheden H., Hindorf C., Engblom H. Appropriate coronary revascularization can be accomplished if myocardial perfusion is quantified by positron emission tomography prior to treatment decision. *J Nucl Cardiol.* 2019 Nov 8 [Epub ahead of print].

Oddstig J., Leide Svegborn S., Almquist H., Bitzén U., Garpered S., **Hedeer F.**, Hindorf C., Jögi J., Jönsson L., Minarik D., Petersson R., Welinder A., Wollmer P., Trägårdh E. Comparison of conventional and Si-photomultiplier-based PET systems for image quality and diagnostic performance. *BMC Med Imaging.* 2019 Oct 22; 19(1):81.

Akil S., **Hedeer F.**, Carlsson M., Arheden H., Oddstig J., Hindorf C., Jögi J., Erlinge D., Engblom H. Qualitative assessment of myocardial ischemia by cardiac MRI and coronary stenosis by invasive coronary angiography in relation to quantitative perfusion by positron emission tomography in patients with known or suspected stable coronary artery disease. *J Nucl Cardiol.* 2018 Dec 10. [Epub ahead of print].

Engblom H., Xue H., Akil S., Carlsson M., Hindorf C., Oddstig J., **Hedeer F.**, Hansen MS., Aletras AH., Kellman P., Arheden H. Fully quantitative cardiovascular magnetic resonance myocardial perfusion ready for clinical use: a comparison between cardiovascular magnetic resonance imaging and positron emission tomography. *J Cardiovasc Magn Reson.* 2017 Oct 19; 19(1):78.

Oddstig J., Hindorf C., **Hedeer F.**, Jögi J., Arheden H., Hansson MJ., Engblom H. The radiation dose to overweighted patients undergoing myocardial perfusion SPECT can be significantly reduced: validation of a linear weight-adjusted activity administration protocol. *J Nucl Cardiol.* 2017 Dec; 24(6):1912-1921.

Akil S., Sunnersjö L., **Hedeer F.**, Hedén B., Carlsson M., Gettes L., Arheden H., Engblom H. Stress-induced ST elevation with or without concomitant ST depression is predictive of presence, location and amount of myocardial ischemia assessed by myocardial perfusion SPECT whereas isolated stress-induced ST depression is not. *J Electrocardiol.* 2016 May-Jun; 49(3):307-15.

Hindorf C., Oddstig J., **Hedeer F.**, Hansson MJ., Jögi J., Engblom H. Importance of correct patient positioning in myocardial perfusion SPECT when using a CZT camera. *J Nucl Cardiol.* 2014 Aug; 21(4):695-702.

Akil S., Al-Mashat M., Hedén B., **Hedeer F.**, Jögi J., Wang JJ., Wagner GS., Warren JW., Pahlm O., Horáček BM. Discrimination of ST deviation caused by acute coronary occlusion from normal variants and other abnormal conditions, using computed

electrocardiographic imaging based on 12-lead ECG. *J Electrocardiol.* 2013 May-Jun; 46(3):197-203.

Oddstig J., **Hedeer F.**, Jögi J., Carlsson M., Hindorf C., Engblom H. Reduced administered activity, reduced acquisition time, and preserved image quality for the new CZT camera. *J Nucl Cardiol.* 2013 Feb; 20(1):38-44.

Soneson H., **Hedeer F.**, Arévalo C., Carlsson M., Engblom H., Ubachs JF., Arheden H., Heiberg E. Development and validation of a new automatic algorithm for quantification of left ventricular volumes and function in gated myocardial perfusion SPECT using cardiac magnetic resonance as reference standard. *J Nucl Cardiol.* 2011 Oct; 18(5):874-85.

Summary

Coronary artery disease, leading to ischemic heart disease and myocardial infarction, is a major cause of mortality and a leading cause of heart failure worldwide. Different cardiac imaging methods are used for detection of myocardial ischemia and infarction as well as assessment of cardiac function, and play an important role for clinical management and decision making in these patients. Myocardial perfusion single-photon emission computed tomography (SPECT) is a widely used nuclear cardiac imaging method for diagnosing ischemic heart disease and myocardial infarction and for assessment of volumes and ejection fraction (EF) of the cardiac left ventricle (LV). Cardiac magnetic resonance imaging (CMR) is another imaging method considered to be the reference method for detection of myocardial infarction and cardiac function. The overall aim of this thesis was to further elucidate the diagnostic performance of myocardial perfusion SPECT (MPS) for detection of myocardial infarction and assessment of cardiac functional parameters, using CMR as the reference method.

Paper I investigated the diagnostic performance of MPS for assessment of LV volumes and LVEF and compared different MPS software, using CMR as the reference method. It was shown that MPS underestimates LV volumes compared to CMR whereas accuracy for assessment of LVEF was better. Precision was low for all measures. There were differences between the MPS software.

Paper II investigated the sensitivity and specificity of MPS with electrocardiography gated technique and a ^{99m}technetium labeled radiotracer for detection of myocardial infarction, using late gadolinium enhancement (LGE) CMR as the reference method. Gated MPS showed high sensitivity and specificity for infarct detection, only missing the smallest infarcts <3% of the LV mass.

Patients with a specific disturbance in the cardiac electrical conduction system, left bundle branch block (LBBB), are known to often have a specific tracer uptake pattern on MPS engaging the LV septal wall, mimicking perfusion defects seen in ischemia and infarction. The underlying pathophysiological mechanisms behind this MPS uptake pattern were investigated in Paper III. The results showed that typical MPS uptake pattern in patients with LBBB were mainly related to regional myocardial dyskinesia and wall thickening rather than myocardial fibrosis, stress-induced ischemia and ECG characteristics.

Paper IV sought to investigate the diagnostic performance of MPS for detection of myocardial infarction and assessment of LV volumes and LVEF, comparing a modern solid-state cadmium-zinc-telluride (CZT) detector gamma camera technique with a conventional gamma camera, using CMR as the reference method. The results showed

a moderate sensitivity and high specificity for detection of infarcts >3% of the LV mass with no difference between the gamma cameras. LV volumes were underestimated compared to CMR with a slightly higher accuracy for the CZT compared to the conventional gamma camera and a relatively large impact on accuracy by the MPS software used.

In summary, the papers of this thesis showed a moderate to high sensitivity and high specificity for MPS to detect myocardial infarctions with no difference between modern and conventional gamma cameras. However, small infarcts were still missed by MPS. LV volumes were underestimated by MPS with low precision whereas accuracy for LVEF was better. The MPS software used had a higher impact on accuracy of LV volume and EF assessment than did type of gamma camera. It might be of value to take these results into consideration when interpreting an MPS study in a clinical setting.

Populärvetenskaplig sammanfattning

Blodet försörjer kroppens olika organ med syre och näringsämnen via kärlsystemet. Hjärtat är kärlsystemets motor. Hjärtmuskeln själv behöver också blodförsörjning för att kunna arbeta, vilken tillgodoses via hjärtats kranskärl. Hos friska personer anpassas blodförsörjningen och syretillförseln efter behovet av syre i olika vävnader. En obalans mellan tillgång och efterfrågan på syre i en vävnad kan dock uppstå. Sådan syrebrist i vävnaden försämrar cellernas och vävnadens funktion och om syrebristen är uttalad och långvarig kan cellerna och delar av vävnaden dö. Även hjärtmuskeln kan drabbas av syrebrist, vanligen till följd av åderförkalkning i hjärtats kranskärl. Syrebrist i hjärtmuskeln försämrar hjärtats funktion och kan ge symptom i form av kärlkramp. Om syrebristen till hjärtmuskeln är uttalad och långvarig kan delar av hjärtmuskeln dö, så kallad hjärtinfarkt.

Inom medicinen finns olika bildgivande metoder för undersökning av hjärtat. Dessa metoder är viktiga verktyg för att kunna ställa korrekt diagnos och sätta in lämplig behandling på en patient med misstänkt hjärtsjukdom. De bildgivande metoderna kan exempelvis undersöka hjärtats pumpförmåga, om hjärtmuskeln har syrebrist och om det finns tecken till ärrvävnad i hjärtat efter en tidigare hjärtinfarkt.

I arbetena i denna avhandling används två bildgivande metoder för undersökning av hjärtat. 1) Vid myokardscintigrafi tar man hjälp av ett radioaktivt ämne och en så kallad gammakamera för att ta bilder av hjärtmuskelns blodflöde och eventuell ärrvävnad i hjärtmuskeln samt för att bestämma hjärtats storlek och pumpförmåga. 2) Vid magnetresonanstomografi (MR) utnyttjar man de magnetiska egenskaperna hos vattnet i kroppen för att generera bilder av hjärtat. För avbildning av hjärtats storlek och funktion samt för avbildning av eventuell ärrvävnad i hjärtat är MR facitmetod.

I avhandlingens delarbete I, II och IV undersöktes hur bra myokardscintigrafi är på att hitta och utesluta ärrvävnad på grund av hjärtinfarkt samt hur bra myokardscintigrafi är på att mäta hjärtats storlek och pumpförmåga. MR användes som facit och undersökningarna utfördes på patienter som kom på remiss på grund av misstänkt hjärtsjukdom. Olika datorprogram som används för bearbetning av hjärtbilderna jämfördes. Dessutom jämfördes om användandet av modern respektive traditionell teknik i myokardscintigrafins gammakamera påverkar mätresultaten. Studieresultaten visar att myokardscintigrafi är ganska bra på att hitta och bra på att utesluta ärrvävnad i hjärtmuskeln, dock finns det risk att missa riktigt små ärr. Vilken gammakamerateknik som användes hade ingen betydelse. Vidare underskattade myokardscintigrafi hjärtats storlek påtagligt medan mätning av hjärtats förmåga att pumpa ut blod var mer rättvisande. Precisionen i mätningarna var låg. Vilken typ av datorprogram som

användes hade ganska stor betydelse för mätresultaten av hjärtats storlek medan typ av gammakamerateknik hade mindre betydelse.

I avhandlingens delarbete III undersöktes en grupp patienter med en särskild störning i det system som leder hjärtats elektriska signaler. Man vet sedan tidigare att patienter med sådan elektrisk störning kan uppvisa ett typiskt utseende på myokardscintigrafibilder som kan likna syrebrist eller ärr efter hjärtinfarkt. Orsakerna till detta typiska utseende är inte helt kända. Resultaten visade att det typiska utseendet på myokardscintigrafi hos patienter med störning i hjärtats elektriska system troligen berodde på hjärtats rörelsemönster och hjärtmuskelns förmåga att förtjocka sig. Det berodde oftast inte på ärrvävnad eller syrebrist i hjärtmuskeln.

Abbreviations

ACS	acute coronary syndrome
ATP	adenosine triphosphate
CABG	coronary artery bypass graft
CAD	coronary artery disease
CCS	chronic coronary syndrome
CCTA	coronary computed tomography angiography
CMR	cardiac magnetic resonance imaging
CT	computed tomography
CZT	cadmium zinc telluride
DE	delayed enhancement
ECG	electrocardiography
Gd	gadolinium
IHD	ischemic heart disease
LBBB	left bundle branch block
LGE	late gadolinium enhancement
LV	left ventricle
LVEDV	left ventricular end-diastolic volume
LVEF	left ventricular ejection fraction
LVESV	left ventricular end-systolic volume
LVSV	left ventricular stroke volume
MI	myocardial infarction
MLEM	maximum likelihood expectation maximization
MPS	myocardial perfusion single-photon emission computed tomography
MR	magnetic resonance
MRI	magnetic resonance imaging
NaI	sodium iodide

NPV	negative predictive value
OSEM	ordered subset expectation maximization
PCI	percutaneous coronary intervention
PET	positron emission tomography
PM	photo multiplier
PPV	positive predictive value
RBBB	right bundle branch block
SPECT	single-photon emission computed tomography
^{99m}Tc	technetium
^{201}Tl	thallium

Introduction

Ischemic heart disease

Ischemic heart disease (IHD) is the number one cause of death worldwide, accounting for more than 9 million deaths (47% women) in 2016 according to the World Health Organization[1,2]. It is also considered the leading cause of heart failure[3,4]. IHD affects both men and women and increases with age[1,2]. In 2010, the global cost of cardiovascular diseases was estimated to more than 850 billion US dollars[5]. Since IHD has a major impact on mortality, morbidity and health care costs globally, improved management of IHD patients is crucial. In this management, different diagnostic testing including cardiac imaging is a corner stone. The studies in this thesis seek to contribute to the field of cardiac imaging and hopefully to be beneficial to patients in the world suffering from IHD.

Pathophysiology

Ischemia and atherosclerosis

Ischemia is defined as an imbalance between oxygen demand and supply in a tissue, for example the myocardium[6]. The most common pathophysiologic process behind ischemia in the myocardium is disease in the coronary arteries (CAD) as an effect of atherosclerosis.

Atherosclerosis is a complex process in the arteries including a number of interacting factors where inflammation seems to play an important role. The inner layer of the arterial wall, the endothelium, is exposed to a large number of factors some of which are stressors affecting the arterial wall in a negative way. These stressors are often associated with known risk factors for CAD such as dyslipidaemia, hypertension, glycated products associated with diabetes, and inflammatory cytokines associated with overweight[7]. The effect of these stressors on the arterial endothelial cells is an increased expression of molecules promoting adhesion of white blood cells. Via inflammatory molecules such as cytokines, more white blood cells will be attracted. The white blood cells migrate into the arterial wall and interact with the endothelial cells and smooth

muscle cells. As a consequence the smooth muscle cells proliferate and generates extra cellular matrix. This mix of white blood cells, proliferating smooth muscle cells and excess of extracellular matrix binds modified lipoproteins and oxidized lipids. In addition, some of the white blood cells transforms to macrophages who start to ingest lipoproteins and lipids turning them into so called foam cells. The end-product of these processes is a growing atherosclerotic lesion or plaque in the arterial wall[7,8], see Figure 1.

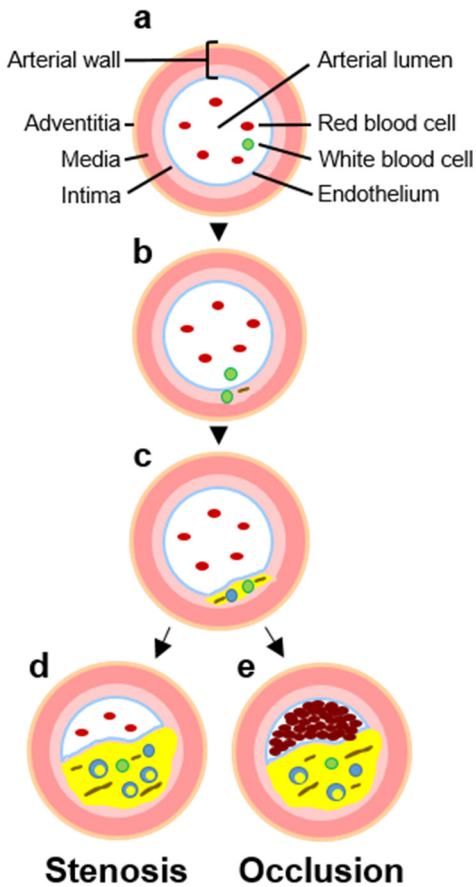

Figure 1. Progression of arterial atherosclerosis. A cross section of a coronary artery. The arterial wall consists of three basic layers. The inner layer is called the intima, contains smooth muscle cells and have a layer of endothelial cells surfacing the blood in the arterial lumen (a). In (b), white blood cells have started to migrate into the arterial wall. They interact with the smooth muscle cells which begin to proliferate and produce extracellular matrix. The white blood cells transforms to macrophages which together with the excess of extracellular matrix binds lipids (c). Some of the macrophages start to ingest lipids transforming them to foam cells. The atherosclerotic plaque continues to grow and an arterial stenosis appears that may reduce the blood flow (d). A rupture of the atherosclerotic plaque will lead to formation of a thrombus that may occlude the artery, leading to acute ischemia and possibly subsequent infarction downstream the occlusion (e).

The atherosclerotic process in CAD probably has a subclinical phase going on for many years, which means that there is a progressive atherosclerotic process going on in the coronary arteries not leading to any symptoms[9]. The clinical presentation of ischemia as a consequence of atherosclerotic CAD mainly occurs in two ways:

1) Growth of an atherosclerotic plaque in a coronary artery with a successive narrowing of the arterial lumen eventually reducing the blood flow, i.e. affecting oxygen supply. Most often this effect becomes evident in situations when oxygen demand increases, i.e. when myocardial work increases for example during exercise. This process is often quite stable or only slowly aggravating and is called stable CAD or as recommended in the new guidelines from European Society of Cardiology (ESC), chronic coronary syndrome (CCS), including both non-obstructive and obstructive CAD[6,7,9].

2) An erosion or rupture of an atherosclerotic plaque leading to formation of a thrombus, acute occlusion of the coronary artery and subsequent acute myocardial ischemia. This process is called acute coronary syndrome (ACS)[6,10-12].

Myocardial ischemia can also occur as a consequence of embolization or spasm in the coronary artery or when oxygen supply for other reasons become low for example in respiratory failure or severe anemia[13].

The ischemic cascade

The ischemic process emanating from the imbalance between oxygen supply and demand is often referred to as the *ischemic cascade*[6], see Figure 2. The ischemic cascade includes a number of myocardial events seen as a consequence of ischemia, eventually leading to cell death and myocardial tissue necrosis – myocardial infarction.

Metabolic alterations. Adenosine triphosphate (ATP) is the compound used for energy demanding processes in the myocardial myocytes. One such important process is maintaining membrane potentials. For effective production of ATP from different energy sources, oxygen is needed – so called aerobic metabolism. In the case of ischemia, the lack of oxygen causes a shift from aerobic to anaerobic metabolism. As a consequence the production of ATP is markedly decreased and there is an imbalance between ATP production and consumption, leading to changes in cellular ionic equilibrium and intracellular acidosis[14].

Diastolic and systolic dysfunction, i.e. impaired relaxation and contractility of the myocardium, is seen as a consequence of ATP depletion, ionic changes and acidosis[14].

Changes in the electrocardiogram (ECG). The most evident changes to the ECG due to ischemia are alterations in the ST-segment[15].

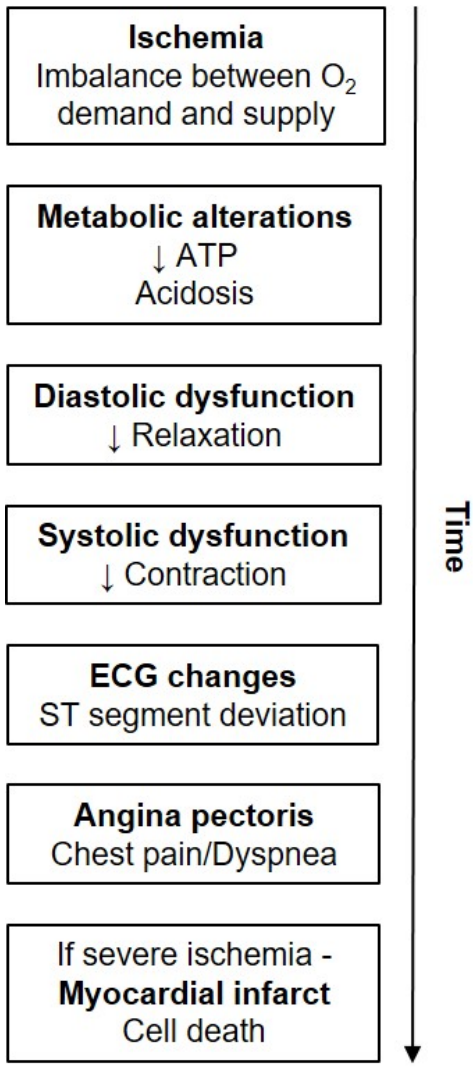

Figure 2. The ischemic cascade. An illustration of the events that occur after onset of myocardial ischemia.

Angina pectoris is the term of the typical symptoms associated with myocardial ischemia. The classic symptom is chest pain, sometimes in conjunction with pain in the back, shoulders, arms, neck and/or jaw. Sometimes pain is not the main symptom of angina pectoris but rather dyspnea.

The term ischemic cascade implies that the events described above is a sequence of events following a specific order, each event leading to the next. However, some authors mean that this is not necessarily the case[16].

Myocardial infarction and heart failure

If the ischemia is severe and persists long enough, the myocytes will eventually be irreversibly damaged and die. Tissue death due to inadequate blood supply, ischemia, is called infarction. The magnitude of cell death in the myocardium is a function of ischemia severity and persistence – the more severe and the longer the ischemia persists, the more myocytes will die. As ischemia duration continues, the infarct typically increases in a wavefront manner from the endocardium to the epicardium and will, if blood supply is not restored, finally affect the full thickness of the myocardium in the area supplied by the affected coronary artery[17]. In addition to the importance of ischemia duration for the final size of the infarcted myocardium, collateral flow from other vessels as well as the localization of the artery occlusion are important factors determining infarct size[18,19]. As the infarcted myocardial tissue heals, the dead cells are replaced by scar tissue[20].

The outcome after an infarction varies and is highly dependent on the size of the infarct. If the blood supply is quickly restored and/or collateral flow and/or localization of artery occlusion are favorable, the final infarct size can be very small and cardiac function totally restored. However, the larger the infarct and myocardial scar, the lower the subsequent cardiac function[21]. If the infarct is large enough to impair cardiac function, the development of heart failure is common. Heart failure can be described as "a progressive disorder that is initiated after an index event… [and] disrupts the ability of the myocardium to generate force, thereby preventing the heart from contracting normally"[22]. An important process involved in the progression of heart failure is myocardial remodeling. Remodeling occurs as a compensation of functional loss, with components such as infarct healing, left ventricular (LV) hypertrophy and dilatation but also myocardial wall thinning and sometimes even aneurysm formation[21].

Clinical management of ischemic heart disease

The clinical presentation of IHD includes a wide range of conditions, from the above mentioned atherosclerotic process in the coronary arteries not giving any symptoms or impairing an individual's life, to the life-threatening condition of acute occlusion of a coronary artery with acute severe ischemia in the myocardium.

Clinically, the acute ischemic condition is referred to as acute coronary syndrome (ACS) whereas the stable obstructive or non-obstructive CAD is referred to as chronic coronary syndrome (CCS) in the latest guidelines[9,11,12]. The distinction between the chronic and acute conditions is not absolute. Rather the CAD is to be seen as a chronic condition lasting for years, with a subclinical phase often developing to a symptomatic phase and possibly with sudden episodes of acute worsening (ACS). Nevertheless, the

disease is most often progressive and serious and clinically have to be managed with diagnostic testing and treatment which overlap between chronic and acute conditions[9].

Diagnosis

The diagnosis of suspected IHD follows a couple of steps that basically can be applied to both chronic and acute conditions, of course with a difference in acuteness of the diagnostic process[9].

First of all, the symptoms of a patient have to be judged of being indicative of IHD or not, most often symptoms of angina pectoris as described above. Secondly, the presence of comorbidities have to be evaluated since they could affect therapeutic decisions. Thirdly, basic testing, including biochemical tests, ECG and often different imaging methods, is used followed by the fourth step which is assessment of clinical likelihood for presence of IHD. The fifth step includes new diagnostic testing based on the likelihood assessment in step four. This step often includes different kind of cardiac imaging methods which is the focus for this thesis and will be discussed in further detail below. The final step is choosing appropriate therapy based on the previous steps.

Therapy

The different treatment options of choice for IHD can basically be divided into three main areas – lifestyle management[23], pharmacological therapy[9,11,12] and revascularization[24]. Pharmacological therapy and revascularization are important areas in both ACS and CCS, whereas lifestyle management is mainly focused upon in the chronic setting.

Healthy lifestyle behaviours are important for prevention of IHD and its consequences[25,26] and include smoking cessation[27], healthy diet[28,29], physical activity[30] and normal weight[31].

Pharmacological therapy in IHD has two aims – reduction of ischemia and angina symptoms and to prevent future cardiovascular events[9]. Important anti-ischaemic drugs include beta-blockers, nitrates and calcium channel blockers. Beta-blockers reduce myocardial oxygen demand by reducing heart rate, contractility and atrioventricular conduction[32]. Nitrates act on symptoms of angina mostly by dilatation of peripheral veins but also by dilatation of peripheral and coronary arteries[32,33]. Calcium channel blockers act mainly by vasodilatation and reduction of peripheral vascular resistance[32]. Event preventing drugs include antiplatelet and anticoagulant drugs, lipid-lowering drugs and drugs affecting the renin-angiotensin-aldosterone system[9]. Antiplatelet drugs prevent the activation and aggregation of platelets whereas anticoagulant drugs prevent the formation and action of thrombin[9]. Lipid-lowering pharmacological therapy aims

to affect the atherosclerotic process by reducing deposition of lipids and lipoproteins in the arterial wall[34]. Angiotensin-converting enzyme inhibitors and angiotensin receptor blockers are drugs affecting the renin-angiotensin-aldosterone system and act by lowering blood pressure and affecting myocardial remodeling, especially in patients with heart failure[9].

Revascularization in the case of ACS aims to restore myocardial perfusion as quickly as possible since time is the main factor affecting how much myocardium will be injured and infarcted. In CCS, the aims with revascularization are reducing angina symptoms and improve prognosis. There are three main methods to obtain revascularization – fibrinolysis by pharmacological intervention, percutaneous coronary intervention (PCI) and coronary artery bypass grafting[24]. Whereas pharmacological fibrinolysis is used only for ACS in some circumstances, PCI is used for both acute and chronic conditions and CABG mainly for chronic conditions but occasionally also in the acute setting.

Cardiac imaging

There are currently several diagnostic methods available for use in patients with known or suspected IHD, many of which are different imaging modalities. The different imaging methods can be divided either into invasive and non-invasive methods or into anatomical and functional methods, respectively. Below, I will describe the methods used in the papers included in this thesis – myocardial perfusion single-photon emission computed tomography (SPECT), cardiac magnetic resonance imaging (CMR) and ECG – with a special focus on myocardial perfusion SPECT (MPS).

Myocardial perfusion SPECT

Myocardial perfusion single-photon emission computed tomography (SPECT) is a non-invasive nuclear medicine technique used to investigate myocardial perfusion and function. Myocardial perfusion SPECT (MPS) uses an intravenously injected radioactive tracer to visualize the myocardium. The radiotracer is distributed in the myocardium ideally in proportion to myocardial perfusion and can be administered both at rest and at stress (exercise or pharmacological). Images are acquired using a gamma camera. By acquiring gamma camera images gated to the ECG, different phases of the cardiac cycle can be imaged, thereby enabling assessment of cardiac function by measuring left ventricular (LV) volumes at end-diastole (ED) and end-systole (ES) as well as left ventricular ejection fraction.

The use of radioactive tracers to study cardiac function began already in the 1920s and myocardial perfusion in the 1960s but it was not until the 1970s the method became clinically available[35].

Radiopharmaceuticals

Radioactive tracers or radiopharmaceuticals are compounds consisting of a radionuclide coupled to a tracer substance. The tracer substance determines which physiological or pathophysiological processes to be visualized and the radionuclide is used for the visualization process – imaging.

In MPS, ^{201}thallium (^{201}Tl) or the ^{99m}technetium (^{99m}Tc) labeled tracers 2-methoxy-isobutyl-isonitrile (^{99m}Tc-sestamibi) and 1,2-bis[bis(2-ethoxyethyl) phosphino] ethane (^{99m}Tc-tetrofosmin) are commonly used radiopharmaceuticals today.

^{201}Thallium is a radionuclide with "built-in" physiological properties. It is biochemically an analogue to potassium, enters the myocardium via the sodium-potassium-ATPase pump mechanism and is distributed in proportion to regional myocardial blood flow. It redistributes over time, a property that can be used to assess myocardial viability[35,36]. Although ^{201}Tl has physiological properties suitable for myocardial perfusion imaging the use is declining due to some limitations. The relatively long half-life (73 hours) gives a high radiation dose to the patient. Because of the radiation dose, injected activity has to be low which impairs image quality, especially for ECG-gated SPECT. The relatively low energy of the emitted photons affects image quality and leads to significant soft tissue attenuation[37]. See Figure 3.

Figure 3. Anterior view of whole body planar scintigraphy with ^{201}thallium (^{201}Tl). Examinations were performed at the Department of Clinical Physiology, Lund University Hospital, in June 1977 to assess the whole body distribution of ^{201}Tl at excerise stress and at rest. At exercise (left image) high tracer uptake is seen especially in the heart and in skeletal muscle, whereas at rest (right image) high tracer uptake is seen especially in the abdominal organs.

Compared to ^{201}Tl, the ^{99m}technetium labeled tracers tetrofosmin and sestamibi have some properties making them more favourable. The half-life of ^{99m}Tc is shorter (6 hours) allowing for larger amounts of injected activity. Furthermore, the energy of the emitted photons is higher. This yields higher image quality, less problems with soft tissue attenuation and greater possibilities to perform ECG-gated SPECT compared to ^{201}Tl, still to a lower radiation burden[37].

The tracers tetrofosmin and sestamibi form lipophilic, cationic complexes. They are taken up by the myocytes in proportion to regional blood flow. The uptake mechanism is not completely understood but is most probably dependent on potential-driven transport where mitochondrial membrane potential seems to play a major role[38-41]. Neither of these two ^{99m}Tc-labeled tracers are associated with any significant redistribution.

It should be stated that even if the myocardial uptake of ^{201}Tl and the ^{99m}Tc labelled tracers is proportional to regional myocardial blood flow, this is not true for all ranges of blood flows. For myocardial blood flows of approximately >2 ml/g/min, tracer uptake doesn't increase linearly to blood flow but is underestimated[42].

Gamma cameras and formation of images

A nuclear medicine tomographic imaging system for single-photon detection relies on three key components – an element that restricts the photons coming from the radiation source (a collimator), an element that detects the photons from the radiation source (a detector) and an algorithm that reconstructs images.

The conventional gamma camera, sometimes referred to as an Anger camera, was developed in the 1950s by the American engineer and biophysicist Hal O. Anger[43,44]. It consists of a lead collimator for restriction of incoming photons. The collimator is mounted on a detector made of a scintillation material, a sodium iodide (NaI) crystal. The energy of a photon that has passed the collimator is deposited in the scintillation crystal. If the energy is high enough, the scintillation crystal will partly convert the energy into a flash of light. The intensity of the flash is proportional to the energy deposited by the gamma ray. In the conventional gamma camera, the flash is then detected by light sensitive detectors, photo multiplier (PM) tubes, behind the scintillation crystal. The PM tube converts the detected flash of light into an electronic pulse proportional to the light intensity. In a conventional gamma camera, many tens of PM tubes are applied to each detector. The output of the PM tubes are used to determine the location of the flash in the scintillation crystal and thereby determining the origin of the radiotracer gamma ray. By applying an energy window, one can choose to account for photons of only a certain spectrum of energy, thereby rejecting for example scattered photons which would increase noise and decrease resolution in the final image. The forming of an image in the computer is based on applying a matrix of points, pixels, in two dimensions and registering the electrical pulses from the PM tubes for different locations in the matrix[35].

The image produced in this way will be a two-dimensional image, i.e. the image will not contain any information of the depth of which the gamma ray originated. To obtain images of a three-dimensional object, such as the heart, one has to use the technique of tomography, which means to produce cross-sectional image planes of a three-dimensional object. In nuclear medicine single-photon imaging this technique is called single-photon emission computed tomography, abbreviated SPECT. The basis of the SPECT technique is to use a number of images of the object acquired from different angles around the object. In a gamma camera this is accomplished by mounting the detectors on a gantry that can be rotated around the object. In modern conventional

gamma cameras, most often two detectors are mounted on the gantry which can be put in different angles of each other and rotated around the object for image acquisition in different angles[35].

The recent decade, a new generation of gamma cameras using solid-state detectors has evolved. Here the NaI crystal in the detectors of a conventional gamma camera has been changed to a detector made of solid-state material, often cadmium-zinc-telluride (CZT). In brief, the main difference between the CZT solid-state detector and the NaI crystal scintillation detector is that the deposited energy of a photon in the solid-state detector is directly converted into an electronic pulse. Hence, PM tubes are not needed, and as a result the energy resolution becomes better. Additionally, the solid-state detectors themselves are arranged into a "matrix", meaning that the localization of the electronic pulse is done directly in the detector and not via the array of PM tubes which is the case in a conventional gamma camera. Another advantage of the new technique is that it makes it possible to construct a gamma camera with optimized geometry, including specific collimation, for example for cardiac dedicated gamma cameras[35]. All together these properties of the CZT gamma cameras yield an improved spatial and energy resolution as well as improved count sensitivity compared to a conventional gamma camera.

The last key component is image reconstruction. There are basically two different principles for image reconstruction in cardiac nuclear imaging, back-projection and iterative techniques. The basic idea behind back-projection is to use all acquired image angles, projections, from the gamma camera. The uptake intensity in each pixel of the matrix is calculated from each image projection. A line is then "back-projected" to a matrix the size of the field-of-view from all acquired image projections, where the intensity of the line is proportional to the uptake intensity along that line. In sites where objects with uptake are situated, the back-projected lines on the matrix will cross and objects with uptake of different intensity will take form. Lastly, the back-projected images are filtered and then ready for software processing and display. The idea behind iterative techniques is to reconstruct an image from successive "guesses" about the true image. The process starts with a guess of every pixel having the same intensity. The guess is then modified for every iteration and will finally converge into the "true" image. Examples of iterative reconstruction methods for myocardial perfusion nuclear imaging are maximum likelihood expectation maximization (MLEM) and ordered subset expectation maximization (OSEM)[35]. See Figure 4.

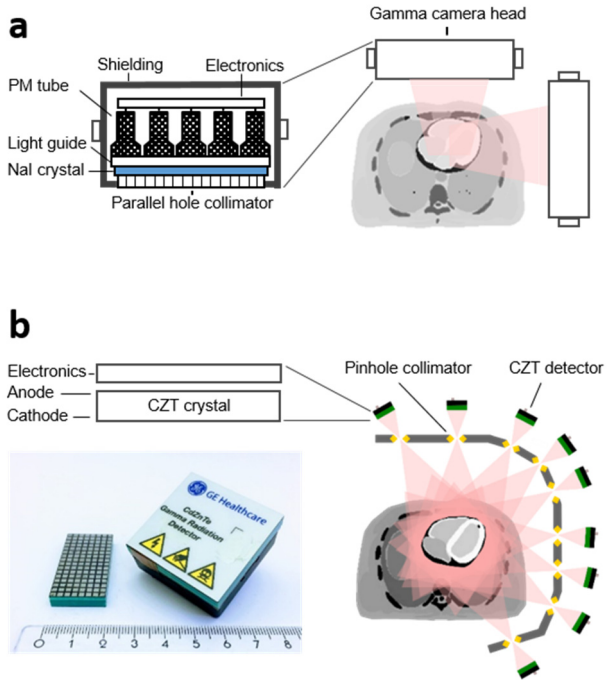

Figure 4. Illustration of the principles of a conventional gamma camera (a) and a solid-state detector gamma camera (b). A cardiac examination in a conventional gamma camera (a) is seen to the right with parallel hole collimator detectors rotating around the object. A schematic illustration of the components of a conventional gamma camera detector is seen to the left. NaI – sodium iodide, PM – photo multiplicator. In (b) a cardiac examination in a solid-state detector gamma camera (GE Discovery NM 530c) is seen. The system has a design based on stationary CZT detectors with pinhole collimation. The detector-pinhole units have a cricular arrangement with a focused field of view of the heart. A schematic illustration of a solid-state detector is seen to the left (upper), and below an image of the CZT detector of the GE Discovery NM 530c system. CZT – cadmium zinc telluride. Illustrations courtesy of Mikael Peterson and Michael Ljungberg.

Examination principles, image processing and interpretation

SPECT is nowadays the standard approach for image acquisition in myocardial perfusion nuclear imaging. As mentioned above, image acquisition in the gamma camera can be performed with ECG triggering, also called gated SPECT. By giving the gamma camera acquisition system information about the cardiac cycle via the patients ECG, time resolved images can be reconstructed. Most often the cardiac cycle is divided into eight or sometimes sixteen intervals (frames/bins). This enables assessment of cardiac function by visual interpretation of myocardial wall motion as well as assessment of volumes and ejection fraction of the left ventricle by automated software processing[37].

Myocardial perfusion SPECT (MPS) image processing is performed with computer software. One of the most important features of such software is an algorithm for

myocardial segmentation which is performed in all cardiac cycle intervals. Primarily only the cardiac left ventricle (LV) is segmented. Furthermore, many software present the LV in standard orientations, most often in short axis view and two long axis views. Many software offers image display in grayscale or different colour scales. Importantly, the standard way to display the images is in relation to the myocardial region with the most intense uptake. This means that the region with most intense uptake is set to the maximum level of the used grayscale/colour scale and all other parts of the LV myocardium is scaled to this maximum uptake. Other features most commonly included in different software packages are ways of automatic quantification of LV volumes and ejection fraction as well as semi-quantification of regional myocardial perfusion[35,45,46].

Myocardial perfusion SPECT is performed both at rest and at stress. Since ischemia depends on a balance between oxygen demand and supply, patients with suspected IHD and significant obstructive CAD are most often planned for MPS examination at both stress and rest. A stress examination is performed to increase cardiac oxygen demand by either exercise or pharmacological stress. Exercise is commonly performed by bicycle ergometer or treadmill. Pharmacological stress uses either vasodilator drugs such as adenosine or regadenosone or drugs that increase cardiac inotropy and chronotropy such as dobutamine and atropine. The MPS radiopharmaceutical is injected intravenously at peak stress (exercise or pharmacological). Images are then acquired in the gamma camera. For a rest examination, the radiopharmaceutical is injected at resting state and images are then similarly acquired. When images are interpreted, the rest and stress examination are compared regarding myocardial perfusion and function. An examination with uniformly distributed perfusion at rest and at stress and with normal functional parameters (LV volumes and ejection fraction) is typically interpreted as a normal examination. A regional perfusion defect present at stress but not at rest is typically a sign of stress-induced ischemia, i.e. there is a balance between myocardial blood demand and supply at rest but an imbalance at stress. A regional perfusion defect present at rest and unchanged at stress is typically a sign of a previous myocardial injury/scar or in some cases a sign of severe ischemia already at rest. See Figure 5 and 6.

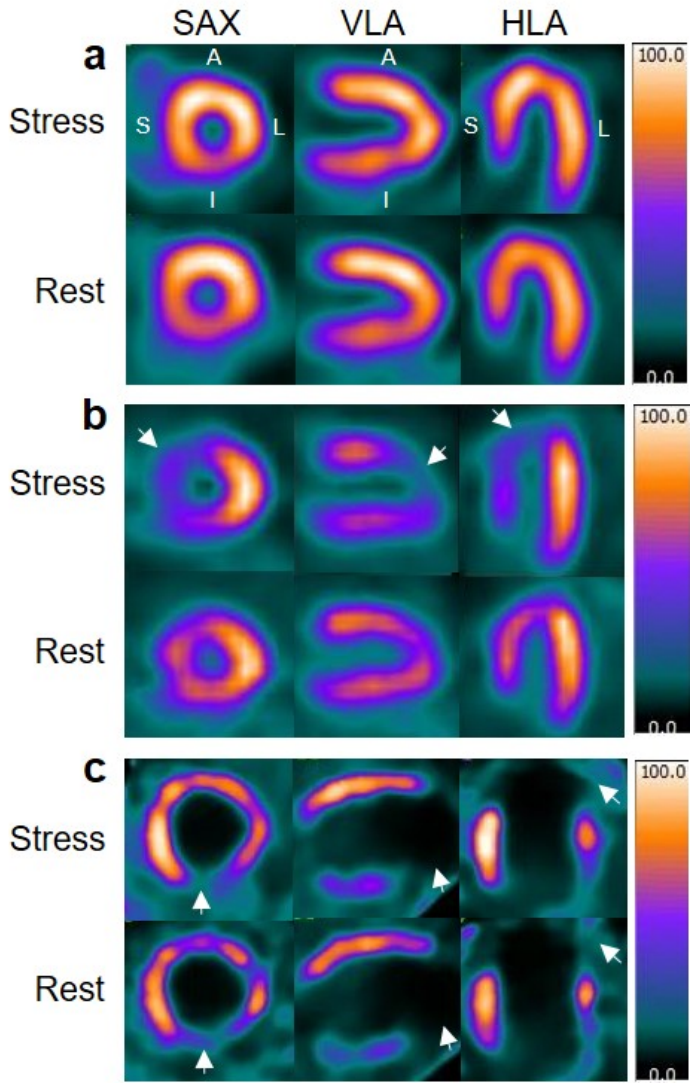

Figure 5. Three cases, (a), (b) and (c), of myocardial perfusion SPECT using ^{99m}Tc-tetrofosmin. Corresponding summed images of the left ventricle at stress (upper row) and at rest (lower row) are shown in short axis view (SAX), vertical long axis view (VLA) and horizontal long axis view (HLA). A – anterior wall, L – lateral wall, I – inferior wall, S – septal wall. Case (a) is an example of a normal examination. The tracer is homogenously distributed similarly at rest and at stress. In case (b), homogenous tracer uptake is seen at rest, whereas decreased uptake is seen in the anteroseptal wall at stress (arrows), as a sign of stress-induced ischemia. In case (c), inhomogenous tracer uptake with absent uptake in the apical and inferior parts of the left ventricle is seen both at rest and stress. This is an example of scar after a myocardial infarction.

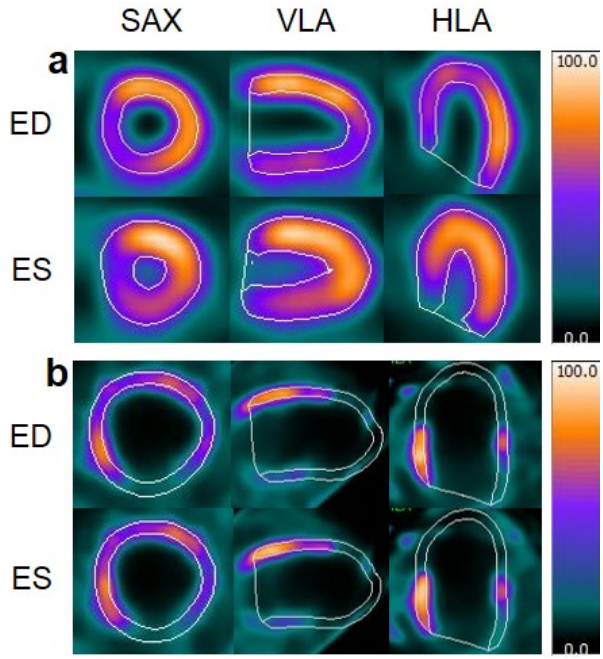

Figure 6. Two cases, (a) and (b), of ECG-gated myocardial perfusion SPECT (MPS) at rest using ^{99m}Tc-tetrofosmin. Corresponding images at end-diastole (ED, upper row)) and end-systole (ES, lower row) are shown in short axis view (SA), vertical long axis view (VLA) and horizontal long axis view (HLA). The thin white lines are the delineation of the epicardial and endocardial left ventricular borders from the automated segmentation algorithm in the MPS software. Case (a) is an example of a normal gated MPS and is the same patient as in case (a) in Figure 5. Note the myocardial wall thickening and increased intensity of the radiotracer as well as the size of the left ventricular cavity in the images at end-systole compared to end-diastole. Case (b) is an example of an enlarged left ventricle with almost no wall thickening and only a minimal change of the left ventricular cavity at end-systole compared to end-diastole as signs of markedly impaired function. This case is the same as case (c) in Figure 5 and the absent tracer uptake as a sign of infarction can also be seen in the gated images.

Magnetic resonance imaging

Magnetic resonance imaging (MRI) is a non-ionizing, non-invasive technique used to acquire images of the human body in any imaging plane.

The technique is based on complex physics. The human body consists, to a large extent, of water. Every water molecule contains two hydrogen atoms. The nucleus of a hydrogen atom have one positively charged proton. The proton spins around its own axis and according to classic physics a charged particle in motion causes a magnetic field. Thus, the proton behaves like a small magnet with two poles. When put into an external magnetic field, the protons align with the external magnetic field and spin with a certain frequency called the Larmor frequency. The Larmor frequency is proportional to the strength of the magnetic field. To be able to detect the protons in a strong magnetic field, as is the case in an MR scanner, one have to change the direction of the

protons' spins. This is accomplished by applying a radio frequency (RF) pulse which is absorbed by the protons and changing the direction of the spins. When the RF pulse ends, the protons again align with the external magnetic field while generating electrical signals. These signals can be detected by the scanner. To localize the origin of the signals, a gradient system is applied causing small variations in the magnetic field. Since the Larmor frequency is proportional to the magnetic field it becomes possible to affect protons by RF pulses in different parts of the body. The different amounts of hydrogen protons and their surrounding molecular environment in different tissues of the human body, make it possible to differentiate between different tissues and organs. Images are generated by mathematical processing of the acquired signals, a process called Fourier transformation[47].

Assessment of myocardial infarction and cardiac function

As was described previously for MPS, image acquisition in cardiac magnetic resonance imaging (CMR) can be performed with ECG triggering. This allows for acquiring MR signals through the cardiac cycle and creating images of the moving heart, cine images, for assessment of cardiac function. Compared with MPS, the spatial and temporal resolution for CMR is significantly higher and CMR is considered the reference method for cardiac functional assessment[48], see Figure 7. Special CMR methods for quantification of regional myocardial function are also available, which uses different ways to quantify deformation (strain) of the myocardial wall[49].

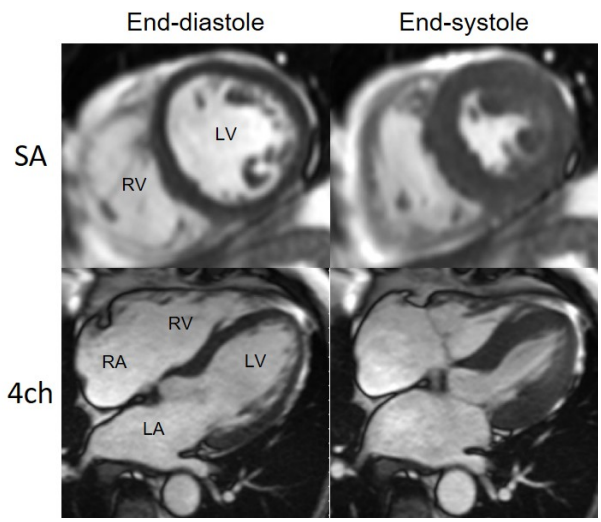

Figure 7. Cine CMR images triggered to the ECG for assessment of cardiac functional parameters such as wall motion, volumes and ejection fraction. Images are shown in short axis view (SA, upper panel) and 4-chamber view (4ch, lower panel). Images at and-diastole to the left and end-systole to the right. LA– left atrium, LV – left ventricle, RA – right atrium, RV – right ventricle.

Sometimes the use of a contrast agent is necessary for MR characterization of specific morphology and tissue properties. Contrast agents based on gadolinium is most commonly used in CMR. Gadolinium (Gd) has paramagnetic properties and is thereby able to affect the MR signal. In CMR, Gd is attached to a carrier molecule that is distributed in the extracellular space. The contrast is injected intravenously and reaches a steady state in the extracellular space after approximately 20 minutes. Thus, the amount of contrast agent in a tissue is proportional to the amount of extracellular space.

The scar tissue of a myocardial infarction (MI) has a larger extracellular volume compared to normal myocardium. Therefore, if a Gd-based contrast agent is injected, the amount of contrast will be higher in the scar tissue compared to the normal myocardium. In infarct imaging with MR, a Gd-based contrast agent is injected and images are acquired after the contrast has reached steady state. Since the amount of contrast agent will differ between scar tissue and normal myocardium, the MR signals will differ between scar and normal myocardium which can be seen in the resulting images. Typically, the MR sequences used for MI imaging try to null the signal from normal myocardium. Normal myocardium will therefore appear black whereas scar tissue will appear hyperenhanced. Hence the terms delayed contrast enhancement (DE) or late gadolinium enhancement (LGE) are used for MI imaging in CMR. CMR is considered the reference imaging method for MI detection in vivo[50], see Figure 8.

In addition, CMR can be used for assessment of myocardial perfusion[51]. Image acquisition is performed simultaneously with the injection of a contrast agent and can be performed both at rest and pharmacological stress. Territories with decreased perfusion will have a decreased in-flow of contrast and therefore a lower MR signal compared to territories with normal perfusion. This technique is referred to as first-pass perfusion imaging.

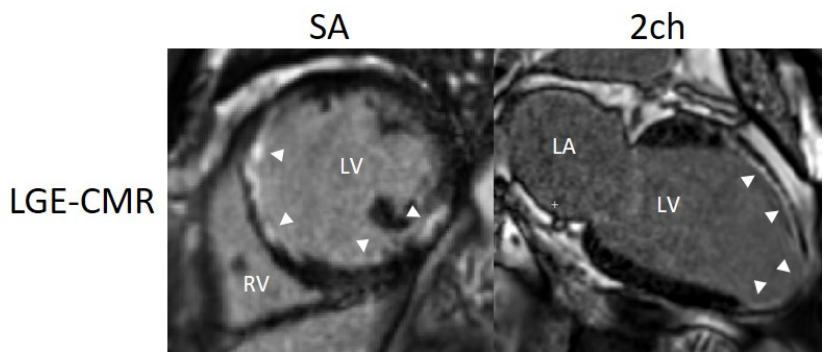

Figure 8. Imaging of a scar after myocardial infarction with late gadolinium enhancement cardiac magnetic resonance (LGE-CMR). Images are shown in short axis view (SA) and 2-chamber view (2ch). Normal myocardium appears black whereas scar tissue appears white (arrows). LA – left atrium, LV – left ventricle, RV – right ventricle.

Electrocardiography

Electrocardiography (ECG) is a non-invasive technique used for graphically depicting the electrical activity of the heart as a function of time. The standard 12-lead ECG is formed by applying 10 electrodes in a specific manner on the human body surface. The output in each lead is a function of the summed electrical vectors measured in that lead. The electrical activation of the heart follows a strict pattern leading to a synchronized way of cardiac motion. The cardiac cycle by ECG is traditionally divided into intervals – P, Q, R, S and T – each defining a specific part of the cardiac electrical cycle. See Figure 9a.

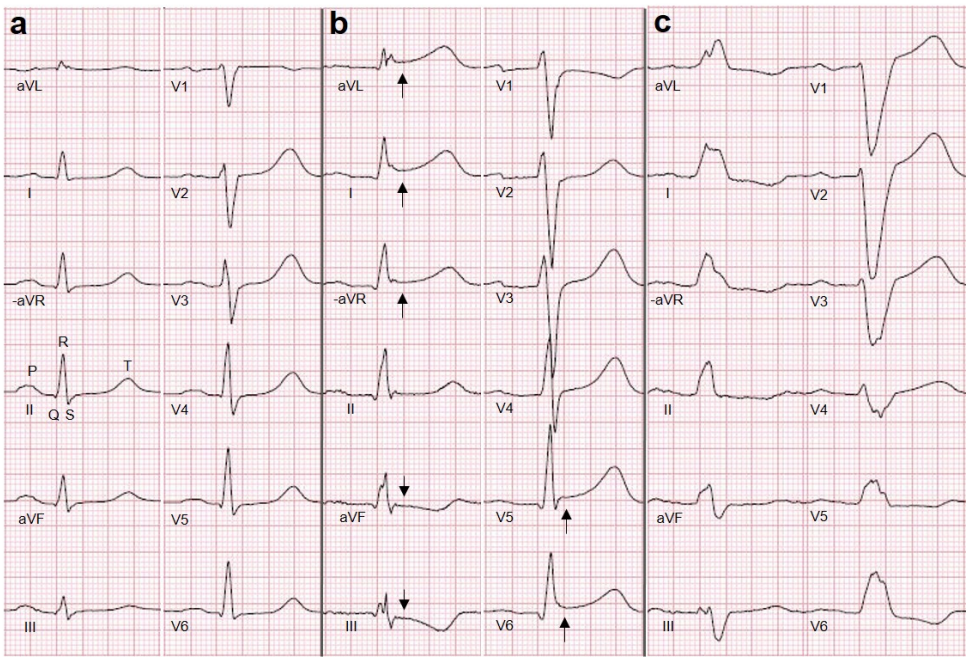

Figure 9. Three examples of 12-lead electrocardiograms (ECG). In (a), a normal ECG is displayed with the different parts of the ECG complex shown in lead II. An ECG with changes of ischemic origin is seen in example (b). Note the changes in the ST segment (arrows). An example of left bundle branch block (LBBB) is seen in (c). The ECG fulfills strict criteria for complete LBBB as suggested by Strauss et al.[52] by increased QRS duration (150 ms), a QS complex in leads V1 and V2, and mid-QRS notching or slurring in leads V5, V6, I and aVL.

ECG in ischemic heart disease

As mentioned previously, myocardial ischemia affects the myocytes and alters their electrical properties. Ischemia causes repolarization disturbances which can be seen in the ST segment of the ECG, an interval representing repolarization of the ventricles. Upon ongoing myocardial ischemia, the ST segment can be depressed or elevated,

depending on the extent and transmurality of the ongoing myocardial ischemia as well as the location. If the ischemia leads to cell injury and myocardial infarction, other changes to the ECG may appear such as alterations in the QRS complex and the T wave. These kind of signs are used in diagnosing IHD by ECG especially in ACS[11,12,53]. See Figure 9b.

Other cardiac electrical alterations that may appear in IHD and myocardial infarction is disturbances in the cardiac electrical conduction system. The cardiac conduction system consists of cells specialized in conducting the electrical signal through the heart to provide a synchronized electrical activation. Under normal conditions, the electrical activity origins in the sinoatrial node. It spreads through the atria and then reaches the atrioventricular node and bundle on its way to the ventricles. On the ventricular side, the conduction system is divided into two main branches, one on the left side and one on the right side, and through them the electrical activity is further spread in the ventricles. Disturbances that may appear in different cardiac conditions, for example in IHD and myocardial infarction, is conduction blockage in the ventricular branches – right bundle branch block (RBBB) and left bundle branch block (LBBB). Right bundle branch block is considered a more benign conduction disturbance compared to LBBB which may cause more profound alterations in the myocardial electrical activation, thus affecting the mechanical properties of the heart[54-56]. The typical effect is uncoordinated or dyssynchronous ventricular contraction leading to inefficient cardiac pumping. However, the effect on cardiac pumping by LBBB differs substantially between patients. LBBB causes typical changes to the ECG. This in turn makes it more difficult to diagnose IHD with ECG since traditional ischemic signs on ECG are not valid. LBBB does not only affect the diagnostic accuracy of IHD by ECG, but may also cause challenges in other diagnostic methods, especially methods for assessment of myocardial perfusion[57]. See Figure 9c.

Other cardiac imaging modalities

In addition to the methods described above there are a number of other imaging methods used to diagnose IHD.

Coronary angiography is an invasive method based on X-rays and an iodine-based contrast agent. It is used to assess the anatomy of the coronary arteries and thus enables the possibility to assess presence and extent of CAD. The major advantage with this method is that it enables diagnostics and intervention (PCI) to be performed in the same session.

Computed tomography (CT) is a non-invasive method using X-rays to produce images of the human body in three dimensions. For diagnosis of IHD this method is mainly

used for non-invasive imaging of the coronary arteries. CT methods for assessment of more functional aspects related to myocardial perfusion are under development, at this date however not widely clinically available[58].

Echocardiography is a non-ionizing, non-invasive imaging method using ultrasound to create images of the heart. It has the ability to describe cardiac anatomy, regional myocardial wall motion and assess velocities such as blood flows[59].

Positron emission tomography (PET) is a non-invasive nuclear medicine imaging technique. Similarly to SPECT, as described previously, it detects the decay of a radioactive tracer designed to assess a specific physiological or pathophysiological process. The PET technique have better spatial and temporal resolution as well as count sensitivity compared to SPECT. Furthermore, for myocardial perfusion assessment, the main advantage of PET compared to SPECT is the superior ability to quantify myocardial perfusion in absolute terms[60].

Usage of cardiac imaging in ischemic heart disease

The use of cardiac imaging methods in ischemic heart disease may have values of different kinds. The first and most obvious is using cardiac imaging to confirm or exclude the suspected diagnosis of IHD. Secondly, cardiac imaging may provide information affecting clinical decision making such as choosing between different treatment options. Thirdly, cardiac imaging may give information about future prognosis. Additionally, different cardiac imaging methods are used in research to gain increased understanding on basic physiological and pathophysiological processes.

Myocardial perfusion SPECT is widely used for diagnostic purposes in patients with known or suspected IHD. Its diagnostic accuracy for stress-induced ischemia has been regularly evaluated with sensitivity and specificity of approximately 70-80 %[61,62]. The diagnostic accuracy of MPS using CZT gamma camera technique has also been evaluated[63]. Choosing optimal therapy for patients with chronic coronary syndrome and suspected myocardial ischemia has been debated during the last decade. Especially after the COURAGE and BARI 2D studies concerning medical therapy alone vs. addition of revascularization, where no obvious benefit was seen with revascularization compared to optimal medical therapy alone[64,65]. It has been shown that using physiology-based diagnostic methods to identify patients for revascularization therapy may be beneficial compared to anatomy-based methods[66,67]. Other studies have shown that imaging of stress-induced ischemia can be used as a gatekeeper to revascularization therapy[68,69]. However, the preliminary results of the ISCHEMIA trial, as

communicated on AHA Scientific Sessions in November 2019, revealed no benefit of revascularization to optimal medical treatment alone in patients with moderate to severe ischemia evaluated by stress cardiac imaging[70]. Thus, further studies on the value of cardiac imaging to guide clinical decision making and treatment are needed.

For prognostic evaluation, there are strong evidence showing that patients with a normal stress MPS examination have a low annual rate of major cardiac adverse events[62,71,72]. Conversely, the risk of major cardiac adverse events increase with increasing perfusion deficit on MPS[71]. Moreover, it has been shown that left ventricular ejection fraction (LVEF) is a predictor of cardiac prognosis, where patients with low LVEF have a higher risk of cardiac death[73].

Compared to the extensive literature on MPS for stress-induced ischemia, data on the diagnostic performance of MPS for detection of myocardial scar are not that extensive. In brief, detection rate for large and/or transmural myocardial infarcts is good whereas detection rate for subendocardial small infarcts is not as good[74]. With regard to prognosis, it has been shown that a fixed defect on MPS, increases the risk for future cardiac events[69]. As previously stated, CMR is considered the reference method for assessment of cardiac function and presence of scar. It has been shown that presence of scar as well as impaired cardiac function on CMR are predictors for future MACE in patients with IHD[75-77]. A special diagnostic challenge are patients presenting with symptoms of myocardial infarction but with non-obstructive coronary arteries (MINOCA). Up to 5-10 % of patients with signs of myocardial infarction may belong to this category[78]. In this category of patients, CMR has the potential to play an important role[79]. This highlights the importance of not only focus on stress-induced ischemia but also on signs of myocardial scar when using cardiac imaging methods.

MPS is one of the non-invasive functional imaging methods recommended in the guidelines for management of patients with chronic coronary syndrome, where the other methods are stress echocardiography, stress CMR and PET for functional assessment and coronary CT angiography (CCTA) for anatomical assessment[9]. In the guidelines, all methods have strong evidence for use in patients with CCS. Thus, it may be challenging for the referring clinician to select the proper imaging method. This is elaborated on in a publication by Knuuti et al.[80], where it is pointed out that different diagnostic methods have different ranges of optimal performance depending on pre-test probability of IHD in an individual patient. Thus, although a number of cardiac imaging methods are recommended with equally strong evidence in guidelines for management of patients with IHD, one method may be preferable compared to another in an individual patient. Further studies on the diagnostic performance of a method and comparison of different cardiac imaging methods are therefore warranted.

Aims

The overall aim of this thesis was to further elucidate the diagnostic performance of myocardial perfusion SPECT (MPS) for detection of myocardial infarction and assessment of cardiac functional parameters. The specific aim of each individual paper was:

Paper I

To explore the diagnostic performance of gated MPS for assessment of left ventricular volumes and ejection fraction, by comparing four different MPS software packages, using CMR as the reference method.

Paper II

To determine the sensitivity and specificity of gated MPS with a ^{99m}Tc-labeled tracer for detection of myocardial infarction, using CMR as the reference method.

Paper III

To explore the underlying pathophysiological mechanisms behind left bundle branch block-related tracer uptake pattern on MPS, by using CMR to assess myocardial fibrosis, regional myocardial wall thickness and wall motion, and by assessing characteristics of the ECG.

Paper IV

To explore the diagnostic performance of gated MPS with a cadmium zinc telluride detector gamma camera compared to a conventional gamma camera for detection of myocardial infarction and assessment of left ventricular volumes and ejection fraction, using CMR as the reference method.

Materials and Methods

Study population and study design

All studies in this thesis were approved by the regional Ethical Review Committee at Lund University. All patients were enrolled at Skåne University Hospital. Written informed consent was obtained from all study participants.

Paper I and II

These two studies prospectively included a total of 119 patients, all having a clinical referral for elective MPS because of known or suspected CCS (Ethical Review Committee permission LU 774-03, 2003-11-19). In addition to an MPS examination, patients were asked to undergo CMR. Patients underwent pharmacological stress with adenosine (n=111) or dobutamine (n=8) in the MR scanner. The MPS radiopharmaceutical was injected intravenously at peak stress followed by injection of MR contrast media. After completion of MR imaging, MPS images were acquired. MPS rest imaging was performed the next day (a 2-day protocol) except for three patients where MPS rest imaging was performed the same day (1-day protocol) for logistical reasons. Seven patients did not complete CMR because of claustrophobia or arrhythmia and were excluded. An additional twelve patients for Paper I and four patients for Paper II had to be excluded because of inadequate image material for further analysis. Thus, for Paper I 100 patients and for Paper II 108 patients could be used for further image analysis.

Paper III

This study included patients enrolled in the larger study "Lundahjärta – en studie av hjärtats form och funktion med olika undersökningsmetoder" (Ethical Review Committee permission LU 741/2004, 2004-12-22), where patients coming with a clinical referral for CMR and/or MPS are prospectively included. Patients from "Lundahjärta" with left bundle branch block (LBBB) who had undergone both CMR

with cine and LGE imaging as well as MPS were retrospectively identified. In total, 23 patients were included.

Paper IV

This study included patients from two study cohorts:

1) The first study cohort (Ethical Review Committee permission LU 2013/4010, 2013-06-19) consisted of patients who had undergone a clinical CMR examination because of known or suspected heart disease. Patients who in the clinical CMR report were judged to have a myocardial scar of ischemic origin were asked to participate and undergo MPS at rest with image acquisition in both a dedicated cardiac solid-state CZT detector gamma camera and a dedicated cardiac conventional gamma camera. Out of 47 included patients 11 were excluded – seven because MPS images from both gamma cameras could not be obtained, one because of inadequate LGE-CMR image quality, one because CMR was performed during the acute phase of myocardial infarction and two because of presence of LBBB which is known to possibly affect the MPS image uptake pattern.

2) The second study cohort (Ethical Review Committee permission 2013/550, 2013-08-22) consisted of a subset of patients from another study (the MYOMER study) in which patients clinically referred for an elective coronary angiography because of known or suspected CCS were included. From the MYOMER study, 37 patients were examined with CMR and MPS with image acquisition in both gamma cameras and could therefore be included.

Thus, images from in total 73 patients could be used for further analysis.

Image acquisition and analysis

MPS

Image acquisition

In all studies, patients were injected intravenously with a weight adjusted dose of ^{99m}Tc-tetrofosmin. Images were acquired with the patient in supine and prone position at stress and in supine position at rest. ECG-gated acquisition was performed using 8 bins per cardiac cycle.

For all patients in Paper I and II and for nine patients in Paper III, image acquisition was performed using a Vertex dual-head gamma camera (ADAC Corporation). Acquisition parameters were: 32 projections over a 180°orbit, 40 seconds per projection, 64×64 matrix and a voxel size of 5×5×5 mm. Maximum likelihood-expectation maximization (MLEM) iterative reconstruction with 12 iterations was used followed by a Butterworth filter with a cut-off frequency of 0.55 and order 5.0.

For all patients in Paper IV, image acquisition was performed in both a CZT gamma camera (Discovery NM 530c, GE Healthcare) and a conventional gamma camera (Ventri, GE Healthcare). In Paper III, seven patients were imaged in GE Discovery NM 530c and seven patients were imaged in GE Ventri. Acquisition parameters for the GE Discovery NM 530c were: acquisition time 480 seconds and a voxel size of 4×4×4 mm. Images were reconstructed using an MLEM algorithm, 40 iterations, Green OSL regularization alpha parameter of 0.51, a beta of 0.3 and post-filtered with a Butterworth filter with a cut-off frequency of 0.37 and a power of 7. Acquisition parameters for the GE Ventri were: 60 projections in a total angular range of 180°, 25 seconds per projection and the detectors in L-mode. Images were reconstructed with a resolution recovery ordered subset expectation maximization (OSEM) algorithm (Evolution, GE Healthcare), 12 iterations, 10 subsets and post-filtered with a Butterworth filter with a cut-off frequency of 0.4 and a power of 10.

Image analysis

Analysis of myocardial infarction was performed by visual analysis in the software QGS/QPS (Cedars-Sinai, Los Angeles, USA). The MPS images were analyzed by two observers in consensus in Paper II and by one observer in Paper IV. A perfusion defect in the summed MPS images at rest with decreased wall thickening in the systolic frames of the gated MPS images was interpreted as infarction. An infarct was located to the left descending artery territory or to the left circumflex/right coronary artery territory. In Paper IV, a quantification of tracer uptake according to the standardized 17-segment model[81] was performed, using a 5-point scale ranging from 0 (normal uptake) to 4 (absent uptake).

Analysis of volumes, ejection fraction and mass of the left ventricle was performed using fully automated algorithms of different MPS software packages. In Paper I four different software were used – QGS/QPS, MyoMetrix (GE Healthcare), Emory Cardiac Toolbox (Emory University Medical Center, Atlanta, USA) and EXINI Heart (Exini diagnostics AB, Lund, Sweden). In Paper II the software QGS/QPS and Segment (Medviso AB, Lund, Sweden) were used.

In Paper III, MPS images were analyzed in QGS/QPS and Segment, respectively. A visual analysis was performed by two observers in consensus. A perfusion defect present at rest and stress involving the septal part of the left ventricle, not reassembling a typical left anterior descending artery distribution, was considered a typical LBBB uptake pattern. In addition, one observer quantified tracer uptake according to the standardized 17-segment model, using a 5-point scale ranging from 0 (normal uptake) to 4 (absent uptake) and summed rest scores (SRS) for the whole left ventricle as well as for the septal and lateral wall were calculated.

CMR

Image acquisition

All patients in Paper I, II and III were examined on a 1.5 T Philips Intera (Best, The Netherlands) MR scanner. In Paper IV, seven patients were examined on the 1.5 T Philips Intera, sixty-three patients on a Siemens Magnetom Aera (Erlangen Germany) and three patients on a Siemens Magnetom Avanto (Erlangen, Germany). For evaluation of cardiac function, cine steady-state free precession (SSFP) short-axis images were acquired for the entire left ventricle (slice thickness 8 mm). Cine images were also obtained in the three standard long-axis planes (2-, 3- and 4-chamber views). For evaluation of myocardial infarction, late gadolinium enhancement (LGE) images were acquired 15 minutes after intravenous administration of a Gd-based contrast agent (0.2 mmol/kg).

Image analysis

For Paper I, image analysis was performed using the software ViewForum (Philips, Best, The Netherlands). For all other analyses the software Segment[82] was used.

For assessment of volumes, ejection fraction and mass of the left ventricle, manual delineation of the endo- and epicardial borders at end-diastole and end-systole was performed. In addition, in Paper III functional assessment was performed by analyzing myocardial radial deformation with strain analysis using the feature tracking module in the software Segment. Also, a visual analysis of regional LV wall motion in 17 segments was performed, where each segment was scored according to a 5-point scale: hyperkinesia, normokinesia, hypokinesia, akinesia and dyskinesia. Assessment of myocardial infarction was performed on the LGE-CMR images. Hyperenhanced regions extending from the endocardium according to typical coronary artery territories were considered myocardial infarction. Infarct size was quantified using Segment[83,84].

ECG

In Paper III, all patients had a 12-lead ECG recorded on either a MEGACART-R (Siemens-Elema, Solna, Sweden) or an EC Sense (Cardiolex, Solna, Sweden). Initial LBBB diagnosis was made by a computer algorithm on EC Sense based on the Glasgow ECG program. All ECGs were then manually analysed for the presence of LBBB using strict criteria as suggested by Strauss et al.[52].

Statistical analyses

Data are generally presented as mean±SD unless otherwise stated. A p-value of <0.05 was considered to indicate statistical significance. Continuous variables were compared using a two-sided t-test, Mann-Whitney U-test or Wilcoxon signed-rank test. ANOVA was used to compare more than two groups. Categorical variables were tested using Fischer's exact test.

Note at Lilla Fiskaregatan, Lund. Photo by Fredrik Hedeer.

Results and Comments

Detection of myocardial infarction (Paper II and IV)

In Paper II and IV we sought to investigate the diagnostic accuracy for detection of myocardial infarction of myocardial perfusion SPECT (MPS) with ECG-gated technique and ^{99m}Tc-labeled radiotracer (Paper II) and if there were any differences between a conventional gamma camera and a gamma camera with solid-state CZT detector technique (Paper IV), using LGE-CMR as the reference method.

In Paper II, 108 patients with a clinical referral for MPS because of known or suspected CCS were examined with ^{99m}Tc-tetrofosmin gated MPS and LGE-CMR. Infarcts were found in 30 patients with CMR and in 31 patients with MPS. The sensitivity, specificity, positive predictive value (PPV) and negative predictive value (NPV) on a per patient basis were 93%, 96%, 90% and 97% respectively. All infarcts >3% of the LV mass by CMR were detected on gated MPS. Three cases were false negative on gated MPS, which corresponded to the smallest infarcts by CMR – 2.3%, 1.9% and 1.8% of the LV mass. See Figures 10 and 11.

In Paper IV, 73 patients were examined with LGE-CMR and ^{99m}Tc-tetrofosmin gated MPS with image acquisition in both a solid-state CZT detector gamma camera and a conventional gamma camera. Thirty-six out of these patients were recruited since they had suspected myocardial infarction in the CMR clinical report. Myocardial infarcts were found in 42 patients by CMR and in 28 patients by both CZT and conventional MPS. Thus, the infarct prevalence was higher in this study population compared to the one in Paper II. The sensitivity, specificity, positive predictive value (PPV) and negative predictive value (NPV) on a per patient basis were 67%, 100%, 100% and 69%. For infarcts >3% of the LV mass by CMR, sensitivity was 82% for CZT MPS and 73% for conventional MPS. See Figure 12.

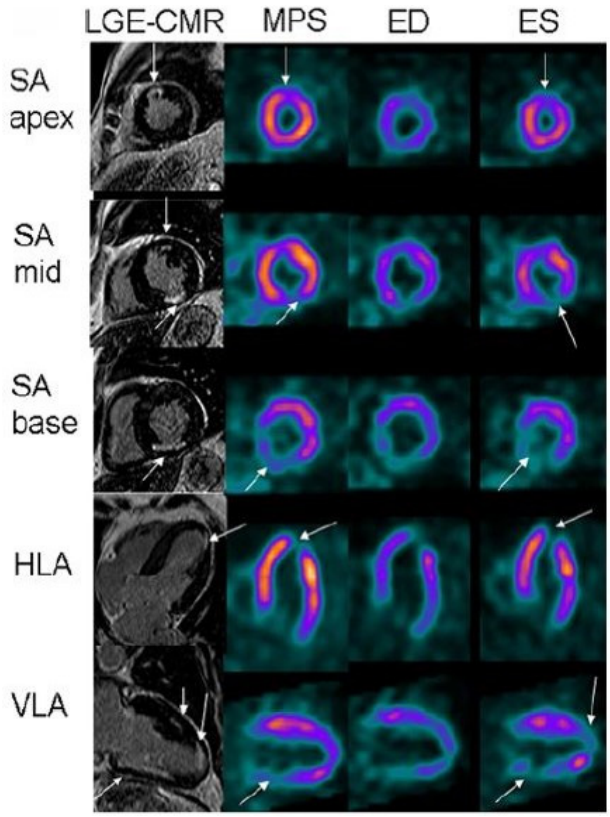

Figure 10. True postive myocardial perfusion SPECT (MPS). One apical/anterior and one inferior infarct, both of which are detected on MPS (arrows). HLA – horizontal long axis, VLA – vertical long axis.

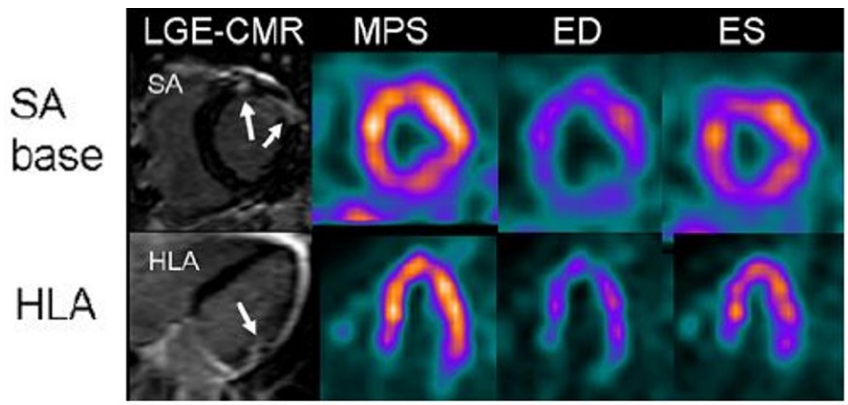

Figure 11. False negative myocardial perfusion SPECT (MPS). On late gadolinium enhancement cardiac magnetic resonance, anterolateral contrast enhancement is seen (arrows) not detected by MPS.

The sensitivity and specificity for infarct detection in Paper II were higher than in previously published studies, also for quite small infarcts[74,85,86]. However, the sensitivity in Paper IV was lower than in Paper II. The main reason for this is probably the larger number of small infarcts in Paper IV compared to Paper II.

In both Paper II and Paper IV specificity was high. This is probably due to assessment of regional wall motion on gated MPS images in conjunction with evaluation of the summed perfusion MPS images. In Paper IV no false positive cases were found on MPS, whereas three patients were false positive in Paper II, two of which had left bundle branch block.

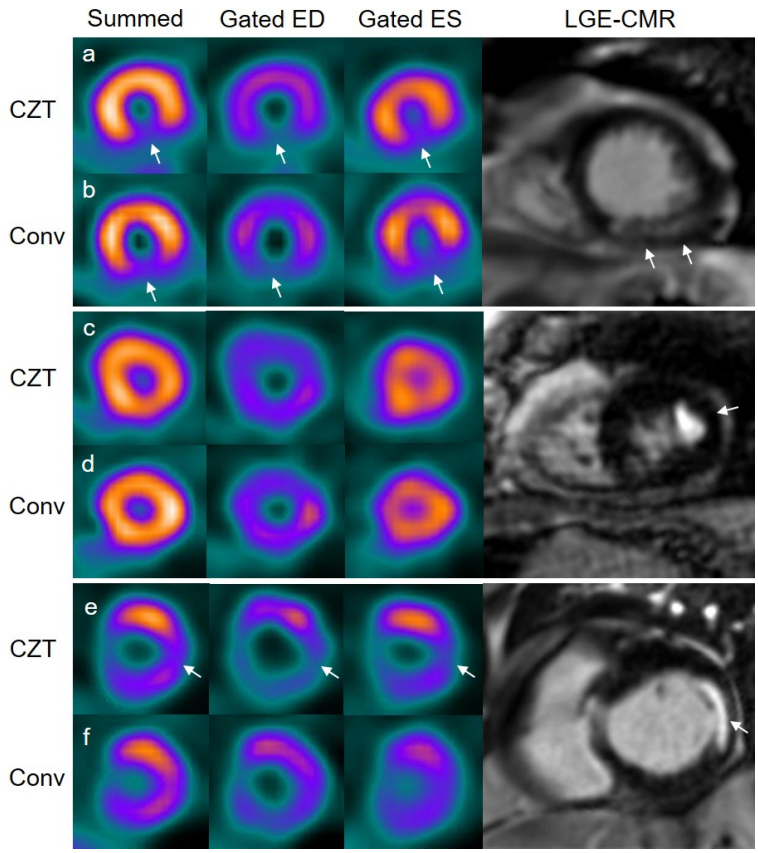

Figure 12. Patient examples of myocardial infarct (MI) by late gadolinium enhancement cardiac magnetic resonance (LGE-CMR), myocardial perfusion SPECT (MPS) with a cadmium zinc telluride (CZT) detector gamma camera and and a conventional gamma camera (Conv). Columns from left to right show summed MPS perfusion images, gated MPS in end-diastole (ED) and end-systole (ES) and LGE-CMR images. Case (a) and (b) are examples of an MI in the apical inferior wall on CMR which is correctly diagnosed by both CZT and conventional MPS (arrows). Case (c) and (d) are examples of an MI in the apical lateral wall on CMR (arrow), missed by both CZT and conventional MPS. Case (e) and (f) are examples of an MI in the basal lateral wall on CMR (arrow) correctly diagnosed by CZT MPS (arrows) but missed by conventional MPS.

Assessment of LV volumes and LVEF (Paper I and IV)

In Paper I and IV, accuracy and precision of gated MPS for assessment of LV volumes and LVEF were investigated, using cine CMR images as the reference method. In Paper I, four different MPS software (QGS/QPS, Emory Cardiac Toolbox, MyoMetrix and EXINI Heart) were compared. In Paper IV, comparison was made between a CZT gamma camera and a conventional gamma camera and in addition two different software (Segment and QGS/QPS).

In Paper I, LV volumes were underestimated by approximately 30% compared to CMR, with some differences between software. For LVEF, accuracy was better. See Figure 13.

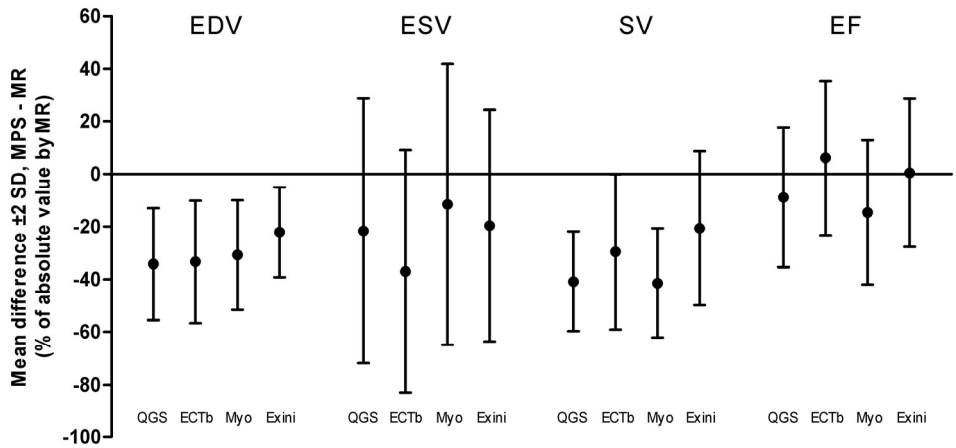

Figure 13. Percent mean bias±2SD for end-diastolic volume (EDV), end-systolic volume (ESV), stroke volume (SV) and ejection fraction (EF) using four different myocardial perfusion SPECT software compared to cardiac magnetic resonance. QGS – QGS/QPS, ECTb – Emory Cardiac Toolbox, Myo – MyoMetrix, Exini – EXINI Heart.

Also in Paper IV LV volumes were significantly underestimated whereas accuracy for LVEF was better compared to CMR. There were significant differences between the CZT and the conventional gamma camera but the absolute values of the differences were small. Differences between software were larger with larger underestimation of LV volumes by QGS/QPS compared to Segment. See Figure 14.

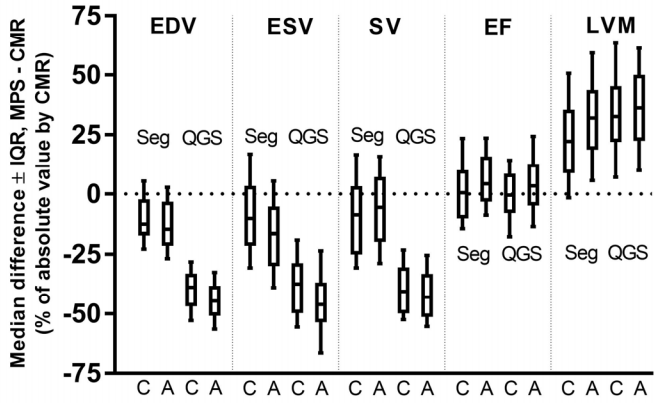

Figure 14. Percent median bias for end-diastolic volume (EDV), end-systolic volume (ESV), stroke volume (SV), ejection fraction (EF) and left ventricular mass (LVM) using MPS with two different gamma cameras (C – cadmium zinc telluride detector gamma camera and A – conventional Anger gamma camera) and two different MPS software (Seg – Segment and QGS – QGS/QPS) compared to cardiac magnetic resonance. Boxes extends from 25th to 75th percentiles and whiskers extends from 10th to 90th percentiles.

In both Paper I and IV, ranges of bias (limits of agreement) for all measures were large, i.e. precision was low.

An important reason for the underestimation of LV volumes by MPS, is the limited spatial resolution associated with the SPECT technique, ranging between 7 and 15 mm[87], as compared to CMR where spatial resolution is approximately 1.5 mm. Temporal resolution in gated MPS is also lower which may play a role[88].

In a clinical perspective, assessment of LVEF by MPS is accurate on a population level, whereas LV volumes are significantly underestimated. Precision is low for all measures. Thus, in an individual patient, MPS values of LV volumes and LVEF should be interpreted cautiously and in conjunction with visual evaluation of gated images. The impact of MPS software on these measures is large whereas impact of different gamma cameras is smaller. When comparing repeated MPS examinations in an individual patient, the same MPS software should be used.

Mechanisms behind typical MPS tracer uptake pattern in patients with LBBB (Paper III)

In Paper III, underlying mechanisms behind LBBB-related tracer uptake pattern on MPS were explored.

Visual evaluation of the MPS images of the 23 patients with LBBB resulted in 13 patients considered to have a tracer uptake pattern on MPS typical of LBBB whereas 10 patients were considered not to have such uptake pattern. For the entire population, summed rest score (SRS) at MPS for the left ventricle ranged from 5 to 20, indicating that the uptake pattern on MPS for a patient with LBBB vary considerably, see Figure 15. Patients with uptake pattern typical of LBBB had higher total SRS and a larger difference in rest score between the septal and lateral wall compared to the patients with no LBBB-typical uptake pattern. One out of 23 patients were considered to have stress-induced ischemia.

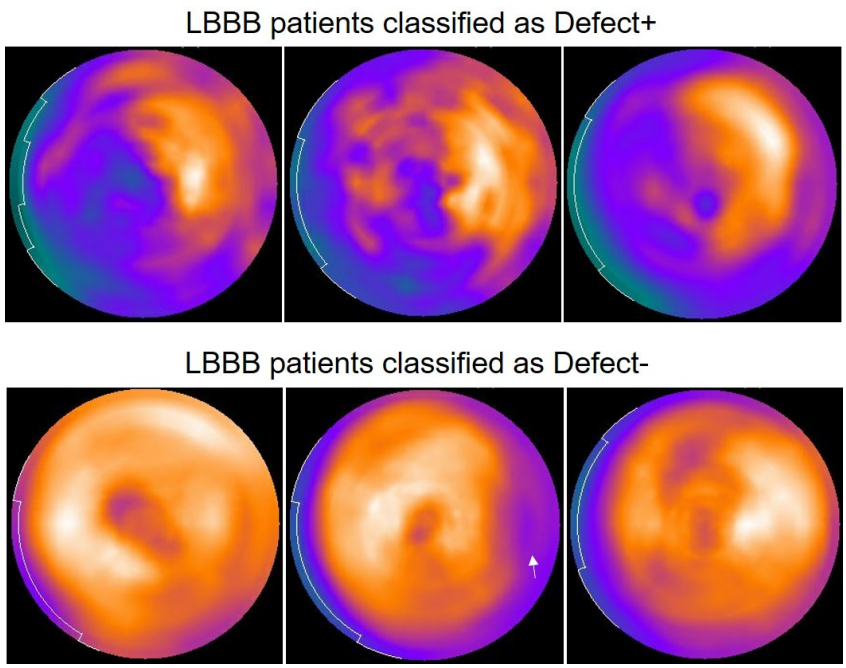

Figure 15. Examples of three patients classified as having a tracer uptake pattern on myocardial perfusion SPECT typical of left bundle branch block (LBBB) (Defect+), upper panel, and three patients classified not to have a typical LBBB tracer uptake pattern, lower panel. Images are so called polar plots of the left ventricle with apex in the middle, anterior wall – upper, lateral wall – right, inferior wall – lower and septal wall – left. The patient in the middle, lower panel, had a myocardial infarct in the lateral wall (arrow) verified by late gadolinium enhancement cardiac magnetic resonance.

Visual assessment of wall motion on CMR images showed a larger proportion of dyskinetic segments in the septal wall combined with a larger proportion of hyperkinetic segments in the lateral wall for patients with LBBB-typical uptake pattern on MPS compared to the patients with no such uptake pattern. There was a relation between myocardial deformation by radial strain on CMR and tracer uptake on MPS, with significantly higher strain values in segments with normal tracer uptake and gradually lower strain values in segments with lower MPS tracer uptake, see Figure 16. Patients with uptake pattern typical of LBBB had significantly thinner septal wall compared to lateral wall whereas no such difference could be seen for patients without LBBB-typical uptake pattern. However, the absolute values of the differences in wall thickness were small and the impact on differences in uptake pattern on MPS seen in this study was therefore probably minor. Six patients were found to have myocardial fibrosis on LGE-CMR but in none of these cases the distribution or extent of fibrosis corresponded to the distribution or extent of uptake defects on MPS. All patients but two fulfilled the strict ECG criteria for LBBB. QRS duration on ECG, a measure of electrical dyssynchrony, did not differ between patients with and without LBBB-typical uptake pattern on MPS.

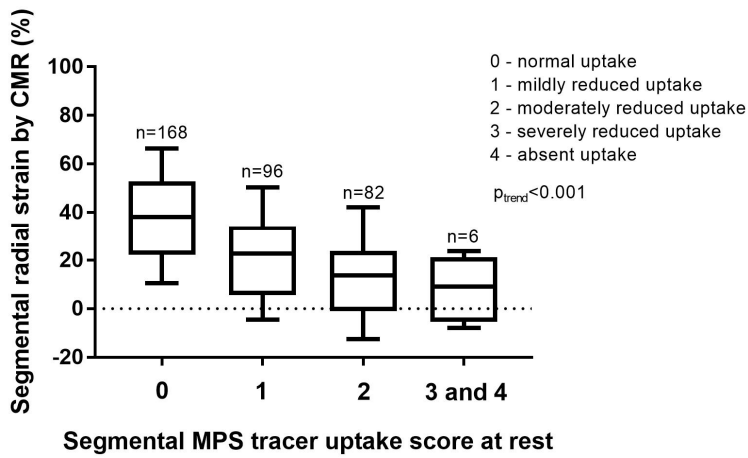

Figure 16. Radial strain on cardiac magnetic resonance (CMR) in each segment according to American Heart Association 17-segment model in all patients, correlated to visual assessment of uptake score in each segment on myocardial perfusion SPECT (MPS). Boxes extends from 25th to 75th percentiles and whiskers from 10th to 90th percentiles.

Conclusions and Future perspectives

- Gated myocardial perfusion SPECT (MPS) with a ^{99m}Tc-labeled tracer has moderate to high sensitivity and high specificity for detection of myocardial infarction compared to the reference method LGE-CMR. There seems to be no significant difference between using a solid-state detector gamma camera compared to a conventional gamma camera (Paper II and Paper IV).
- Gated MPS systematically underestimates left ventricular (LV) volumes by approximately 20-40% compared to the reference method CMR, depending on which MPS software used. A solid-state detector gamma camera is slightly more accurate than a conventional gamma camera. For assessment of LV ejection fraction, the accuracy for MPS is better. Precision for all measures is low (Paper I and Paper IV).
- Presence of typical tracer uptake pattern on MPS in patients with LBBB, is mainly related to regional myocardial dyskinesia and wall thickening rather than myocardial fibrosis, stress-induced ischemia or ECG characteristics (Paper III).

Gated myocardial perfusion SPECT was shown to have moderate to high sensitivity and high specificity for detection of myocardial infarcts compared to CMR. However, for small infarcts, <3% of the LV mass, the sensitivity of MPS was low. As previously described, even a small myocardial infarct as assessed by CMR has a negative impact on patient prognosis[75]. On the other hand, data on MPS show a good prognosis for patients with normal MPS findings[71,89,90]. Thus, prospective studies looking at prognosis with regard to presence of myocardial infarction in patients undergoing both MPS and LGE-CMR are warranted. Does prognosis differ between patients where there are discrepancies between MPS and LGE-CMR with regard to presence of myocardial infarction, and patients where MPS and LGE-CMR agree?

Another question that arises, pertain to reconstruction of MPS images. The chosen reconstruction parameters might be a trade-off to be able to interpret all different pathophysiological parameters assessed by MPS, such as ischemia, infarction and function. However, optimal MPS reconstruction may differ between different

pathophysiological parameters, which opens up for future studies on reconstruction optimization. Also, the studies on assessment of LV volumes and ejection fraction reveal differences in MPS software which might be related to different implemented algorithms for LV segmentation. This opens up for future studies on optimization of LV segmentation in MPS software.

The mechanisms behind typical MPS perfusion pattern in patients with LBBB were studied in a small number of patients. Investigation of these hypotheses in studies with prospective inclusion of larger study populations are needed.

Afoot and light-hearted I take to the open road,
Healthy, free, the world before me,
The long brown path before me leading wherever I choose.

Walt Whitman, *Song of the Open Road*

Acknowledgements

No man is an *Iland*, intire of itselfe
Every man is a peece of the *Continent*,
a part of the *maine*

John Donne, *Meditation XVII – Devotions Upon Emergent Occasions*

Without the help and support from a lot of people, this thesis would not exist. I want to thank all of you and express special gratitude to the following:

My supervisor **Henrik Engblom**, for your support of all kinds, for your patience, for fruitful discussions, for your openness, for your good-temperedness, for many laughs and for being a good friend.

My co-supervisor **Håkan Arheden**, for always taking time to listen, for asking questions and for teaching me the value of reflection.

My co-supervisor **Marcus Carlsson**, for your expertise, for always being honest and for teaching me the importance of diligence.

All colleagues in the Cardiac MR group, for your willingness to help, for being open-minded and for creating a world class research environment. **Shahnaz Akil** for your tremendous work with the MYOMER study.

My boss **Jonas Jögi** for support and trust.

My **physician colleagues at the clinic** – you are the reason why I go to work with joy every morning. **Bo Hedén**, for putting up with me as a roomie during all these years – *Jaså?!*

Techs, secretaries, nurses and all other colleagues at the clinic, for help and for creating a great work atmosphere – *Klinfys-andan*.

Cecilia Hindorf and **Jenny Oddstig**, for your expertise in radiation physics and your patience with me asking the same questions over and over again.

Region Skåne, **Hjärt-Lungfonden** and **Svenska Läkaresällskapet** for helping fund my research.

My mother, **Bodil**, my deceased father, **Rolf**, and my sister, **Kristina**, for always being there.

My wife, **Anna**, for loving me, supporting me and being there for me in the best of times as well as the worst of times. Our daughters, **Ebba** and **Signe** – you're simply the best!

förvåna dig själv idag
oberedd
vandra där isen är svag
orädd
utmana naturens lag
oklädd
bejaka ditt inre jag
oledd

Ola Bengtsson – *Förvåna dig själv idag* ur *andra sökandet 1999-2000*

References

1. Global Health Estimates 2016: Deaths by Cause, Age, Sex, by Country and by Region, 2000-2016. Geneva, World Health Organization; 2018. 2018.
2. Nowbar AN, Gitto M, Howard JP, Francis DP, Al-Lamee R. Mortality From Ischemic Heart Disease. *Circ Cardiovasc Qual Outcomes.* 2019;12(6):e005375.
3. Fox KF, Cowie MR, Wood DA, et al. Coronary artery disease as the cause of incident heart failure in the population. *Eur Heart J.* 2001;22(3):228-236.
4. Gheorghiade M, Sopko G, De Luca L, et al. Navigating the crossroads of coronary artery disease and heart failure. *Circulation.* 2006;114(11):1202-1213.
5. Bloom DE, Cafiero, E.T., Jané-Llopis, E., Abrahams-Gessel, S., Bloom, L.R., Fathima, S., Feigl, A.B., Gaziano, T., Mowafi, M., Pandya, A., Prettner, K., Rosenberg, L., Seligman, B., Stein, A., & Weinstein, C. The Global Economic Burden of Non-communicable Diseases. Geneva: World Economic Forum. 2011.
6. Nesto RW, Kowalchuk GJ. The ischemic cascade: temporal sequence of hemodynamic, electrocardiographic and symptomatic expressions of ischemia. *Am J Cardiol.* 1987;59(7):23c-30c.
7. Libby P, Theroux P. Pathophysiology of coronary artery disease. *Circulation.* 2005;111(25):3481-3488.
8. Sakakura K, Nakano M, Otsuka F, Ladich E, Kolodgie FD, Virmani R. Pathophysiology of atherosclerosis plaque progression. *Heart Lung Circ.* 2013;22(6):399-411.
9. Knuuti J, Wijns W, Saraste A, et al. 2019 ESC Guidelines for the diagnosis and management of chronic coronary syndromes. *Eur Heart J.* 2020;41(3):407-477.
10. Crea F, Libby P. Acute Coronary Syndromes: The Way Forward From Mechanisms to Precision Treatment. *Circulation.* 2017;136(12):1155-1166.
11. Ibanez B, James S, Agewall S, et al. 2017 ESC Guidelines for the management of acute myocardial infarction in patients presenting with ST-segment elevation: The Task Force for the management of acute myocardial infarction in patients presenting with ST-segment elevation of the European Society of Cardiology (ESC). *Eur Heart J.* 2018;39(2):119-177.
12. Roffi M, Patrono C, Collet JP, et al. 2015 ESC Guidelines for the management of acute coronary syndromes in patients presenting without persistent ST-segment elevation: Task Force for the Management of Acute Coronary Syndromes in Patients Presenting

without Persistent ST-Segment Elevation of the European Society of Cardiology (ESC). *Eur Heart J.* 2016;37(3):267-315.

13. Thygesen K, Alpert JS, Jaffe AS, et al. Fourth universal definition of myocardial infarction (2018). *Eur Heart J.* 2019;40(3):237-269.
14. Gourdin M. D, P. Impact of Ischemia on Cellular Metabolism. In: Artery Bypass. In: Aronow WS, ed.: IntechOpen; 2013.
15. Bayés de Luna AF-S, M. *The Surface Electrocardiography in Ischaemic Heart Disease: Clinical and Imaging Correlations and Prognostic Implications.*: Wiley-Blackwell; 2007.
16. Maznyczka A, Sen S, Cook C, Francis DP. The ischaemic constellation: an alternative to the ischaemic cascade-implications for the validation of new ischaemic tests. *Open heart.* 2015;2(1):e000178.
17. Reimer KA, Jennings RB. The "wavefront phenomenon" of myocardial ischemic cell death. II. Transmural progression of necrosis within the framework of ischemic bed size (myocardium at risk) and collateral flow. *Lab Invest.* 1979;40(6):633-644.
18. Charney R, Cohen M. The role of the coronary collateral circulation in limiting myocardial ischemia and infarct size. *Am Heart J.* 1993;126(4):937-945.
19. Persson E, Palmer J, Pettersson J, et al. Quantification of myocardial hypoperfusion with 99m Tc-sestamibi in patients undergoing prolonged coronary artery balloon occlusion. *Nucl Med Commun.* 2002;23(3):219-228.
20. Reimer KA, Jennings RB. The changing anatomic reference base of evolving myocardial infarction. Underestimation of myocardial collateral blood flow and overestimation of experimental anatomic infarct size due to tissue edema, hemorrhage and acute inflammation. *Circulation.* 1979;60(4):866-876.
21. Pfeffer MA, Braunwald E. Ventricular remodeling after myocardial infarction. Experimental observations and clinical implications. *Circulation.* 1990;81(4):1161-1172.
22. Mann DL. *Pathophysiology of Heart Failure. In: Braunwald's Heart Disease: A Textbook of Cardiovascular Medicine.* 9 ed: Elsevier Saunders; 2011.
23. Piepoli MF, Hoes AW, Agewall S, et al. 2016 European Guidelines on cardiovascular disease prevention in clinical practice: The Sixth Joint Task Force of the European Society of Cardiology and Other Societies on Cardiovascular Disease Prevention in Clinical Practice (constituted by representatives of 10 societies and by invited experts)Developed with the special contribution of the European Association for Cardiovascular Prevention & Rehabilitation (EACPR). *Eur Heart J.* 2016;37(29):2315-2381.
24. Neumann FJ, Sousa-Uva M, Ahlsson A, et al. 2018 ESC/EACTS Guidelines on myocardial revascularization. *Eur Heart J.* 2019;40(2):87-165.
25. Booth JN, 3rd, Levitan EB, Brown TM, Farkouh ME, Safford MM, Muntner P. Effect of sustaining lifestyle modifications (nonsmoking, weight reduction, physical activity, and mediterranean diet) after healing of myocardial infarction, percutaneous

intervention, or coronary bypass (from the REasons for Geographic and Racial Differences in Stroke Study). *Am J Cardiol.* 2014;113(12):1933-1940.

26. Chow CK, Jolly S, Rao-Melacini P, Fox KA, Anand SS, Yusuf S. Association of diet, exercise, and smoking modification with risk of early cardiovascular events after acute coronary syndromes. *Circulation.* 2010;121(6):750-758.
27. Critchley JA, Capewell S. Mortality risk reduction associated with smoking cessation in patients with coronary heart disease: a systematic review. *JAMA.* 2003;290(1):86-97.
28. Miller V, Mente A, Dehghan M, et al. Fruit, vegetable, and legume intake, and cardiovascular disease and deaths in 18 countries (PURE): a prospective cohort study. *Lancet.* 2017;390(10107):2037-2049.
29. Wang X, Ouyang Y, Liu J, et al. Fruit and vegetable consumption and mortality from all causes, cardiovascular disease, and cancer: systematic review and dose-response meta-analysis of prospective cohort studies. *BMJ.* 2014;349:g4490.
30. Bruning RS, Sturek M. Benefits of exercise training on coronary blood flow in coronary artery disease patients. *Prog Cardiovasc Dis.* 2015;57(5):443-453.
31. Khan SS, Ning H, Wilkins JT, et al. Association of Body Mass Index With Lifetime Risk of Cardiovascular Disease and Compression of Morbidity. *JAMA cardiology.* 2018;3(4):280-287.
32. Rousan TA, Mathew ST, Thadani U. Drug Therapy for Stable Angina Pectoris. *Drugs.* 2017;77(3):265-284.
33. Nossaman VE, Nossaman BD, Kadowitz PJ. Nitrates and nitrites in the treatment of ischemic cardiac disease. *Cardiol Rev.* 2010;18(4):190-197.
34. Mach F, Baigent C, Catapano AL, et al. 2019 ESC/EAS Guidelines for the management of dyslipidaemias: lipid modification to reduce cardiovascular risk. *Eur Heart J.* 2020;41(1):111-188.
35. Iskandrian AE, Garcia, E. V. *Nuclear Cardiac Imaging: Priciples and Applications.* 4 ed: Oxford University Press; 2008.
36. Dilsizian V, Perrone-Filardi P, Arrighi JA, et al. Concordance and discordance between stress-redistribution-reinjection and rest-redistribution thallium imaging for assessing viable myocardium. Comparison with metabolic activity by positron emission tomography. *Circulation.* 1993;88(3):941-952.
37. Hesse B, Tagil K, Cuocolo A, et al. EANM/ESC procedural guidelines for myocardial perfusion imaging in nuclear cardiology. *Eur J Nucl Med Mol Imaging.* 2005;32(7):855-897.
38. Dahlberg ST, Leppo JA. Myocardial kinetics of radiolabeled perfusion agents: basis for perfusion imaging. *J Nucl Cardiol.* 1994;1(2 Pt 1):189-197.
39. Piwnica-Worms D, Kronauge JF, Chiu ML. Uptake and retention of hexakis (2-methoxyisobutyl isonitrile) technetium(I) in cultured chick myocardial cells.

Mitochondrial and plasma membrane potential dependence. *Circulation.* 1990;82(5):1826-1838.

40. Sinusas AJ, Shi Q, Saltzberg MT, et al. Technetium-99m-tetrofosmin to assess myocardial blood flow: experimental validation in an intact canine model of ischemia. *J Nucl Med.* 1994;35(4):664-671.
41. Wackers FJ, Berman DS, Maddahi J, et al. Technetium-99m hexakis 2-methoxyisobutyl isonitrile: human biodistribution, dosimetry, safety, and preliminary comparison to thallium-201 for myocardial perfusion imaging. *J Nucl Med.* 1989;30(3):301-311.
42. Rosenbaum AF, McGoron AJ, Millard RW, et al. Uptake of seven myocardial tracers during increased myocardial blood flow by dobutamine infusion. *Invest Radiol.* 1999;34(2):91-98.
43. Anger HO. Use of a gamma-ray pinhole camera for in vivo studies. *Nature.* 1952;170(4318):200-201.
44. Anger HO. Scintillation Camera. *Rev Sci Instrum.* 1958;29(1):27-33.
45. Germano G, Kavanagh PB, Chen J, et al. Operator-less processing of myocardial perfusion SPECT studies. *J Nucl Med.* 1995;36(11):2127-2132.
46. Fransson H. *Methods for quantitative analysis of myocardial perfusion SPECT: validated with magnetic resonance imaging, phantom studies and expert readers.*: Centre for Mathematical Sciences, Lund University; 2012.
47. Bogaert J, Dymarkowski, S., Taylor, A. M., Muthurangu, V. *Clinical Cardiac MRI.* 2 ed: Springer; 2012.
48. Grothues F, Smith GC, Moon JC, et al. Comparison of interstudy reproducibility of cardiovascular magnetic resonance with two-dimensional echocardiography in normal subjects and in patients with heart failure or left ventricular hypertrophy. *Am J Cardiol.* 2002;90(1):29-34.
49. Chitiboi T, Axel L. Magnetic resonance imaging of myocardial strain: A review of current approaches. *J Magn Reson Imaging.* 2017;46(5):1263-1280.
50. Carlsson M, Arheden H, Higgins CB, Saeed M. Magnetic resonance imaging as a potential gold standard for infarct quantification. *J Electrocardiol.* 2008;41(6):614-620.
51. Engblom H, Xue H, Akil S, et al. Fully quantitative cardiovascular magnetic resonance myocardial perfusion ready for clinical use: a comparison between cardiovascular magnetic resonance imaging and positron emission tomography. *J Cardiovasc Magn Reson.* 2017;19(1):78.
52. Strauss DG, Selvester RH, Wagner GS. Defining left bundle branch block in the era of cardiac resynchronization therapy. *Am J Cardiol.* 2011;107(6):927-934.
53. Herring N, Paterson DJ. ECG diagnosis of acute ischaemia and infarction: past, present and future. *QJM.* 2006;99(4):219-230.
54. Fahy GJ, Pinski SL, Miller DP, et al. Natural history of isolated bundle branch block. *Am J Cardiol.* 1996;77(14):1185-1190.

55. Hardarson T, Arnason A, Eliasson GJ, Palsson K, Eyjolfsson K, Sigfusson N. Left bundle branch block: prevalence, incidence, follow-up and outcome. *Eur Heart J.* 1987;8(10):1075-1079.

56. Smiseth OA, Aalen JM. Mechanism of harm from left bundle branch block. *Trends Cardiovasc Med.* 2019;29(6):335-342.

57. Chareonthaitawee P, Askew, J. W., Arruda-Olson, A. M. *Stess testing in patients with left bundle branch block or paced ventricular rythm.* UpToDate; 2020.

58. Conte E, Sonck J, Mushtaq S, et al. FFRCT and CT perfusion: A review on the evaluation of functional impact of coronary artery stenosis by cardiac CT. *Int J Cardiol.* 2020;300:289-296.

59. Olsson A. *Ekokardiografi.* Ultraview; 2015.

60. Saraste A, Kajander S, Han C, Nesterov SV, Knuuti J. PET: Is myocardial flow quantification a clinical reality? *J Nucl Cardiol.* 2012;19(5):1044-1059.

61. Danad I, Szymonifka J, Twisk JWR, et al. Diagnostic performance of cardiac imaging methods to diagnose ischaemia-causing coronary artery disease when directly compared with fractional flow reserve as a reference standard: a meta-analysis. *Eur Heart J.* 2017;38(13):991-998.

62. Underwood SR, Anagnostopoulos C, Cerqueira M, et al. Myocardial perfusion scintigraphy: the evidence. *Eur J Nucl Med Mol Imaging.* 2004;31(2):261-291.

63. Nudi F, Iskandrian AE, Schillaci O, Peruzzi M, Frati G, Biondi-Zoccai G. Diagnostic Accuracy of Myocardial Perfusion Imaging With CZT Technology: Systemic Review and Meta-Analysis of Comparison With Invasive Coronary Angiography. *JACC Cardiovasc Imaging.* 2017;10(7):787-794.

64. Boden WE, O'Rourke RA, Teo KK, et al. Optimal medical therapy with or without PCI for stable coronary disease. *N Engl J Med.* 2007;356(15):1503-1516.

65. Frye RL, August P, Brooks MM, et al. A randomized trial of therapies for type 2 diabetes and coronary artery disease. *N Engl J Med.* 2009;360(24):2503-2515.

66. Pijls NH, Fearon WF, Tonino PA, et al. Fractional flow reserve versus angiography for guiding percutaneous coronary intervention in patients with multivessel coronary artery disease: 2-year follow-up of the FAME (Fractional Flow Reserve Versus Angiography for Multivessel Evaluation) study. *J Am Coll Cardiol.* 2010;56(3):177-184.

67. Tonino PA, De Bruyne B, Pijls NH, et al. Fractional flow reserve versus angiography for guiding percutaneous coronary intervention. *N Engl J Med.* 2009;360(3):213-224.

68. Hachamovitch R, Hayes SW, Friedman JD, Cohen I, Berman DS. Comparison of the short-term survival benefit associated with revascularization compared with medical therapy in patients with no prior coronary artery disease undergoing stress myocardial perfusion single photon emission computed tomography. *Circulation.* 2003;107(23):2900-2907.

69. Hachamovitch R, Rozanski A, Shaw LJ, et al. Impact of ischaemia and scar on the therapeutic benefit derived from myocardial revascularization vs. medical therapy among patients undergoing stress-rest myocardial perfusion scintigraphy. *Eur Heart J.* 2011;32(8):1012-1024.

70. Hochman JS. for the ISCHEMIA trial. Presented at AHA Scientific Sessions 2019; Nov 16, 2019; Philadelphia, Pennsylvania. In.

71. Otaki Y, Betancur J, Sharir T, et al. 5-Year Prognostic Value of Quantitative Versus Visual MPI in Subtle Perfusion Defects: Results From REFINE SPECT. *JACC Cardiovasc Imaging.* 2020;13(3):774-785.

72. Shaw LJ, Hage FG, Berman DS, Hachamovitch R, Iskandrian A. Prognosis in the era of comparative effectiveness research: where is nuclear cardiology now and where should it be? *J Nucl Cardiol.* 2012;19(5):1026-1043.

73. Hachamovitch R, Rozanski A, Hayes SW, et al. Predicting therapeutic benefit from myocardial revascularization procedures: are measurements of both resting left ventricular ejection fraction and stress-induced myocardial ischemia necessary? *J Nucl Cardiol.* 2006;13(6):768-778.

74. Wagner A, Mahrholdt H, Holly TA, et al. Contrast-enhanced MRI and routine single photon emission computed tomography (SPECT) perfusion imaging for detection of subendocardial myocardial infarcts: an imaging study. *Lancet.* 2003;361(9355):374-379.

75. Kwong RY, Chan AK, Brown KA, et al. Impact of unrecognized myocardial scar detected by cardiac magnetic resonance imaging on event-free survival in patients presenting with signs or symptoms of coronary artery disease. *Circulation.* 2006;113(23):2733-2743.

76. Kwong RY, Sattar H, Wu H, et al. Incidence and prognostic implication of unrecognized myocardial scar characterized by cardiac magnetic resonance in diabetic patients without clinical evidence of myocardial infarction. *Circulation.* 2008;118(10):1011-1020.

77. Peterzan MA, Rider OJ, Anderson LJ. The Role of Cardiovascular Magnetic Resonance Imaging in Heart Failure. *Cardiac failure review.* 2016;2(2):115-122.

78. Pasupathy S, Air T, Dreyer RP, Tavella R, Beltrame JF. Systematic review of patients presenting with suspected myocardial infarction and nonobstructive coronary arteries. *Circulation.* 2015;131(10):861-870.

79. Dastidar AG, Baritussio A, De Garate E, et al. Prognostic Role of CMR and Conventional Risk Factors in Myocardial Infarction With Nonobstructed Coronary Arteries. *JACC Cardiovasc Imaging.* 2019;12(10):1973-1982.

80. Knuuti J, Ballo H, Juarez-Orozco LE, et al. The performance of non-invasive tests to rule-in and rule-out significant coronary artery stenosis in patients with stable angina: a meta-analysis focused on post-test disease probability. *Eur Heart J.* 2018;39(35):3322-3330.

81. Cerqueira MD, Weissman NJ, Dilsizian V, et al. Standardized myocardial segmentation and nomenclature for tomographic imaging of the heart. A statement for healthcare professionals from the Cardiac Imaging Committee of the Council on Clinical Cardiology of the American Heart Association. *Circulation.* 2002;105(4):539-542.

82. Heiberg E, Sjogren J, Ugander M, Carlsson M, Engblom H, Arheden H. Design and validation of Segment--freely available software for cardiovascular image analysis. *BMC Med Imaging.* 2010;10:1.

83. Engblom H, Tufvesson J, Jablonowski R, et al. A new automatic algorithm for quantification of myocardial infarction imaged by late gadolinium enhancement cardiovascular magnetic resonance: experimental validation and comparison to expert delineations in multi-center, multi-vendor patient data. *J Cardiovasc Magn Reson.* 2016;18(1):27.

84. Heiberg E, Ugander M, Engblom H, et al. Automated quantification of myocardial infarction from MR images by accounting for partial volume effects: animal, phantom, and human study. *Radiology.* 2008;246(2):581-588.

85. Andrade JM, Gowdak LH, Giorgi MC, et al. Cardiac MRI for detection of unrecognized myocardial infarction in patients with end-stage renal disease: comparison with ECG and scintigraphy. *AJR Am J Roentgenol.* 2009;193(1):W25-32.

86. Catalano O, Moro G, Cannizzaro G, et al. Scar detection by contrast-enhanced magnetic resonance imaging in chronic coronary artery disease: a comparison with nuclear imaging and echocardiography. *J Cardiovasc Magn Reson.* 2005;7(4):639-647.

87. Imbert L, Poussier S, Franken PR, et al. Compared performance of high-sensitivity cameras dedicated to myocardial perfusion SPECT: a comprehensive analysis of phantom and human images. *J Nucl Med.* 2012;53(12):1897-1903.

88. Germano G, Kiat H, Kavanagh PB, et al. Automatic quantification of ejection fraction from gated myocardial perfusion SPECT. *J Nucl Med.* 1995;36(11):2138-2147.

89. Edenbrandt L, Ohlsson M, Tragardh E. Prognosis of patients without perfusion defects with and without rest study in myocardial perfusion scintigraphy. *EJNMMI research.* 2013;3:58.

90. Hachamovitch R, Berman DS, Kiat H, Cohen I, Friedman JD, Shaw LJ. Value of stress myocardial perfusion single photon emission computed tomography in patients with normal resting electrocardiograms: an evaluation of incremental prognostic value and cost-effectiveness. *Circulation.* 2002;105(7):823-829.

Printed by Media-Tryck, Lund 2020 NORDIC SWAN ECOLABEL 3041 0903

FACULTY OF MEDICINE

Department of Clinical Physiology

Lund University, Faculty of Medicine
Doctoral Dissertation Series 2020:72
ISBN 978-91-7619-934-3
ISSN 1652-8220